ABSTRACT

SUMANASINGHE, SHANTHA RAMANI. **CYTOPLASMIC Ca^{2+} CHANGES IN NEMATODE TREATED *Lotus japonicus* ROOT HAIRS**. (Under the direction of Dr. Nina Strömgren Allen.)

Nitrogen fixation by Rhizobia and phosphorous extraction by Mycorrhiza, are specific plant microbe interactions that are of paramount economical and ecological importance. Of similar impact to the economy and ecology is the interaction between endoparasitic nematodes and plant roots that leads to major losses in crop production. While Nod factor induced signaling events have been a research focus for many years, the nature of the early responses induced by nematode invasion are just beginning to emerge. Recent reports provide morphological as well as physiological and genetic evidence that symbiotic rhizobia and parasitic nematodes use common signaling pathways in the host plant during induction of feeding sites. One of the earliest physiological responses to Nod factors comprises calcium influx at the tip of the root hair and elevation of cytosolic calcium followed after 10 min by calcium spiking over the nucleus. It was therefore of particular interest to investigate whether similar calcium changes occur after treatment with nematodes. I used the ratiometric cytosolic calcium indicator Indo-1, in conjunction with confocal laser scanning microscopy, to monitor calcium changes in *L. japonicus* root hairs in space and time before and after treatment with RKN *Meloidogyne incognita*. The results were compared with those I obtained in parallel experiments after Nod factor application under the same experimental conditions. I showed that treatment with nematodes increases cytoplasmic calcium at the root hair tip by about 263 nM. The response starts about 2 min after RKN were introduced to the chamber and calcium elevation was sustained over a period of at least 20 min. The calcium concentration also

increased over the nuclear area by about 183 nM showing a similar time course, however, calcium spiking was not observed. These results indicate that RKN and Nod factors induce a similar elevation of cytoplasmic calcium levels at the root and provide further evidence of the existence of a common signaling pathway between symbiotic rhizobia, mycorrhiza and parasitic nematodes.

CYTOPLASMIC Ca^{2+} CHANGES IN NEMATODE TREATED *Lotus japonicus* ROOT HAIRS

by
SHANTHA RAMANI SUMANASINGHE

A thesis submitted to the Graduate Faculty of
North Carolina State University
in partial fulfillment of the
requirements for the Degree of
Master of Science

BOTANY

Raleigh

2005

APPROVED BY:

Dr. Wendy F. Boss Member of Advisory Committee	Dr. David McK. Bird Member of Advisory Committee

Dr. Nina Strömgren Allen
Chair of Advisory Committee

DEDICATION

This thesis is dedicated to my loving parents who have always inspired me to reach higher goals in my life.

BIOGRAPHY

I was born in Welimada, Sri Lanka, a beautiful small town geographically located in a basin surrounded by a ring of blue mountains. I was the seventh in my family with four brothers and two sisters. After my primary and secondary education in Central College, Welimada, I entered the Faculty of Science at the University of Peradeniya, Sri Lanka in 1994. I selected my major as chemistry after a competitive general science qualifying exam at the end of the first year. I earned my Bachelor of Science Degree specializing in Chemistry from the Department of Chemistry in 1998. After graduation, I joined the same department as a demonstrator where I conducted tutorial classes and laboratory sessions in general chemistry for undergraduate students. In early 1999, my interest in research led me to join Industrial Technology Institute (ITI), one of the leading research organizations in Colombo, Sri Lanka. As a research assistant at ITI, I was involved in post harvest technology research investigating antifungal compounds present in the fruit peels and leaves of Rambutan (*Nephelium lappacium Linn.*). In the year 1999, I got married to my beloved husband Ruwan Sumanasinghe who is from Maharagama, Sri Lanka. In pursuit of higher studies, we both arrived in the USA in the year 2000.

ACKNOWLEDGEMENT

The work in this study would not have been possible without the guidance, advice and help from the persons mentioned below. I am forever indebted to my parents for bringing me up through many hardships, properly guiding me and showing me the correct pathway for my education. I extend my immense gratitude to my brothers and sisters who were always there to give me advice and a helping hand. I am very thankful to my husband, Ruwan who has always been there for me with his support and love.

I cannot appreciate enough my advisor Dr. Nina S. Allen, whose vast knowledge, experience and guidance has made my graduate studies easier. Without her guidance and prompt advice this study would not have been successful. I am truly grateful to my committee members Dr. Wendy F. Boss and David McK. Bird for being always there to give encouraging remarks and critically reviewing my research.

My special thanks go to Dr. Eva Johannes and my friend Ravisha Weerasinghe for their promptness and guidance, which greatly helped me throughout various parts of my research.

I also would like to offer my deepest appreciation to members of the Bird lab and the Phytrotron for providing me technical assistant throughout this study.

My thanks also go to the Department of Botany for providing financial support for my graduate program.

TABLE OF CONTENTS

LIST OF FIGURES

LIST OF TABLES

LIST OF ABBREVIATIONS

Abbreviation	Definition
µg	Microgram
µl	Microliter
µm	Micrometer
µM	Micromolar
CAM	Calmodulin
CCD	Charge Coupled Device
CDPK	Calcium Dependent Protein Kinase
CFP	Cyan Fluorescence Protein
DCLP	Dichroic Long Pass
DIC	Differential Interference Contrast
DMSO	Dimethylsulfoxide
DNA	Deoxyribonucleic acid
FRET	Fluorescence Resonance Energy Transfer
GFP	Green Fluorescent Protein
hr	Hour
IAA	Indole Acetic Acid
J2	Second stage juvenile nematodes (s)
KDa	Kilo-Dalton
M	Molar
Mas	Mastoporan
MES	2-Morpholinoethanesulfonic acid
min	Minute
ml	Milliliter
mM	Millimolar
mm	Millimeter
MT	Microtubule
NFR	Nod Factor Receptor
nm	Nanometer
PA	Phosphatidic acid
pH	Negative log of the hydrogen ion concentration
RKN	Root Knot Nematode
s	Second

UI	Universal Imaging
UV	Ultra Violet
YFP	Yellow Flourescence Protein

1. INTRODUCTION

1.1. Overlapping regulatory pathway shared by symbiotic Mycorrhiza, rhizobia and parasitic nematodes

Plants interact with both beneficial and harmful biotrophic organisms in the environment. Arbuscular mycorrhiza and rhizobial symbiosis are examples of intracellular, mutually beneficial interactions that extract phosphorous from soil and fix nitrogen in the atmosphere by fungi and bacterial rhizobia, respectively. Among many parasitic associations, the root knot nematode (RKN) plant interaction is one of the most harmful and successful interactions (Trudgill and Blok, 2001).

A common factor for both these parasitic and symbiotic associations is that they penetrate the plant surface using different mechanisms and making their own living space inside parts of the host plants. To obtain food from the plant, these organisms change themselves as well as the interacting plant part. During the rhizobia-legume symbioses, host specific rhizobia initiate a special structure called a nodule, which they use as a nitrogen-fixing site in host legumes after differentiating into bacteroids (Brewin 1999; Crespi and Galvez, 2000). The plant provides the photosynthate in return for the nitrate from bacteria (Esseling et al. 2003). Arbuscular mycorrhiza also forms a symbiotic interaction with most plants. As in rhizobial symbiosis, mycorrhizal fungal hyphae penetrate the plant root epidermis and grow into the root cortex as a highly branched network of hypha called arbuscules. Mycorrhiza extract phosphate from the soil and provide it to the plant through the arbuscule, while getting the photosynthate for its development **(**Harrison, 1999; Brundrett, 2002). Similarly endoparasitic

RKNs form anatomically somewhat similar special feeding structures called root knot galls in most vascular plants (Bird, 1973). Root knot nematodes differentiate into the pear shaped non-migratory form after migrating to the feeding site inside the plant root (Williamson and Gleason, 2003).

Recent studies have demonstrated the possibility of a common signal transduction pathway induced by symbiotic rhizobia, mycorrhiza and the parasitic nematodes during feeding site induction (Koltai et al. 2001; Favery et al. 2002; Kistner and Parniske, 2002; Weerasinghe et al. 2005). Nodule development is a well-studied process and the signal molecules, Nod factors, produced by rhizobia that initiate this process have been identified (Lerogue et al. 1990; Ardourel et al. 1994). In contrast, the signal molecules that induce nematode feeding sites have not been identified but have been proven to act at a distance from the plant (Weerasinghe et al. 2005). Koltai et al. (2001) showed that two early mitogenic nodulation genes, ENOD40 and the cell cycle gene CCS52a are induced in the galls challenged by the RKN *M. incognita* in *Medicago truncatula*. In *M. truncatula,* two transcription regulators, PHAN and KNOX, which are necessary for meristem establishment and known to be expressed in tomato giant cells are also expressed in giant cells induced by *M. incognita* and nodules induced by *Sinorhizobium meliloti* (Koltai et al. 2001). Changes in both actin and microtubule cytoskeleton were similar spatially and temporally with respect to Nod factor and nematode applications (Weerasinghe et al. 2003; Weerasinghe et al. 2005). Similar to Nod factor treated root hairs, nematode treated root hairs in *L. japonicus* showed waviness and branching (Weerasinghe et al. 2005). The Nod factor receptor mutants *nfr1*, *nfr5* and *symRK* had a reduced number of gall formations after Nod factor application, which

indicates that the early transcription initiation processes are similar in the giant cell formation and nodule development. All these observations collectively lead to a common pathway of arbuscule root knot gall and nodule formation by mycorrhiza, RKNs and rhizobia. Ion fluxes are the earliest responses of root hair cells to Nod factors (Allen et al. 1994, Felle et al. 1998; Lhuissier et al. 2001). Calcium influx at the root hair tip occurs first, within seconds of the application of Nod factor to root hairs of *M. sativa* (Felle et al. 1998). After a few seconds of calcium influx, chloride ion efflux (Felle et al. 1998) occurs resulting in plasma membrane depolarization (Ehrhardt et al. 1992: Felle et al. 1995; Kurdjian, 1995) followed by efflux of K^+ (Felle et al. 1998) and rapid intracellular alkalinization of (0.2 - 0.3 pH units) the cytoplasm in *M. sativa* (Felle et al. 1996: Felle et al. (1998). Calcium spiking over the nucleus was observed after about 10 min at one minute intervals in *L. japonicus and M. sativa* (Ehrhardt et al. 1996; Harris et al. 2003). Ion movements resulting from interactions between parasitic nematodes and plants have not been investigated. Since RKNs have been shown to produce a signal acting at a distance (Weerasinghe et al. 2005) that causes cytoskeletal rearrangements and a series of developmental changes in the plant including similar gene expression and giant cell formation, it is obvious to ask the question: "What changes occur in the cytoplasm of receptive root hair cells shortly after nematode addition?" Then with that knowledge it is possible to compare the changes occurring in roots after Nod factor or RKN application to the roots.

1.2. Purpose of research

I have chosen to study the time course of changes in the cytoplasmic calcium concentration in growing root hairs of the model legume *L. japonicus* after nematode addition using various ratio-imaging microscopic methods. According to the literature, calcium appears to be a crucial step in the signaling pathways leading to the Nod factor induced changes. The results obtained with nematode challenge in this study will be compared and contrasted to the responses observed in *L. japonicus* to Nod factors as reported in the literature and recorded during my experiments reported here.

2. REVIEW OF LITERATURE

2.1. Nodule development

2.1.1. Nod genes

The flavonoids present in root excretions of the legumes induce genes in gram-negative soil bacteria, rhizobia. These bacterial genes are collectively called "*nod*" (nodulation) genes or nodulins and are essential for nodule initiation (Fisher and Long, 1992; Downie and Walker, 1999; Cullimore et al. 2001). The nod genes produce signal molecules called Nod factors (Dénarié et al. 1992; Fisher and Long, 1992). The *nodABC* categorized as common nod genes are present in all rhizobial genera, *Azorhizobium*, *Bradyrhizobium*, *Mesorhizobium, Rhizobium, Senorhizobium* and produce the lipochito-oligosaccharide core of Nod factors (Spaink et al. 1991). Mutations in these genes results in an inability to initiate nodules and as a result do not show any of the plant responses that are normally observed during nodulation. Different rhizobia species have specific nod genes that are responsible for the host specificity (Roche et al. 1991; Spaink et al. 1991).

2.1.2. Nod factors

Rhizobial secretions, which include lipochito-oligosaccharides or Nod factors, play a major role in nodule initiation and differentiation (Ardourel et al. 1994; Downie and Walker, 1999; Esseling and Emons, 2003; Horvath et al. 1993; Journet et al. 1994). The molecular dialogue between rhizobia and its specific legume partner via Nod factors, leads to the formation of the root nodule. Lerogue et al. (1990**)** first characterized the Nod factors as "lipochito-oligosacharides". The Nod factors consist of β-1,4-linked tetramers or pentamers of D-

glucosamine residues (Roche et al. 1991; Ardourel et al. 1994). Species-specific Nod factors differ from each other due to the type and position of different molecular substituents linked to the main lipochito-oligosaccharide core (Spaink et al. 1991; Hirsch et al. 2001). These substituents are mainly fatty acyl groups (Spaink et al. 1991: Fisher and Long, 1992).

2.1.3. Plant perception of Nod factor signal

It has been implied that several plant receptors should be present for identification of the nod signal because a host plant may perceive different Nod factors. This is supported by the observation that very low concentrations of Nod factor in the nanomolar range or less are able to induce changes in the host plant (Downie and Walker. 1999). A symbiotic receptor like kinase, SYMRK, is the first molecularly characterized receptor gene in the common mycorrhizal and rhizobial symbiotic pathway (Stracke et al. 2002). However, *Lotus* plants with a mutation in this gene still had the ability to perceive the Nod factor signal and show early changes associated with nodulation. This evidence shows that the perception of bacterial signal is mediated through several receptors. Recently identified Nod factor receptor genes, NFR1 and NFR5 from *Lotus japonicus* show mycorrhizal colonization in mutant plants but do not show any response to rhizobia in mutant *nfr1* and *nfr5* plants (Schauser et al. 1998**)**. Radutoiu et al. (2003) demonstrated that these putative Nod factor receptor genes, NFR1 and NFR5, were necessary for Nod factor perception and acted upstream of genes such as SYMRK in a common pathway. Evidence for receptor mediated function of the Nod factor perception also comes from physiological studies (Felle et al. 1998).

2.1.4. Early changes observed during nodule signal transduction

The process of nodule formation by rhizobia initiates a series of physiological and morphological changes in legume plants (Figure 2.1)

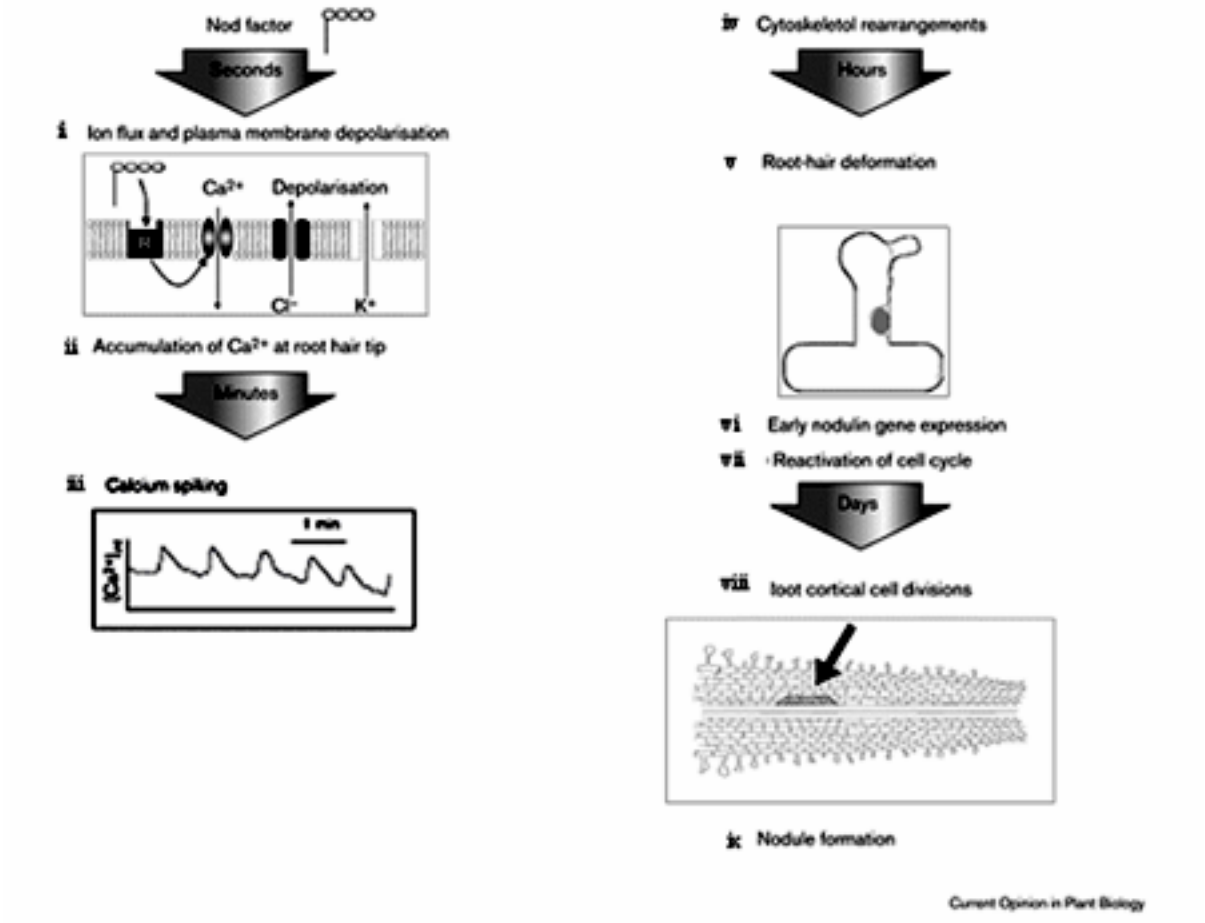

Figure 2.1 Temporal order of plant responses to Nod factors for a 'typical' legume (Modified from Downie and Walker (1999).

As mentioned earlier the earliest physiological change detected after addition of Nod factor involves depolarization of the plasma membrane in root hair cells (Ehrhardt et al. 1992; Felle et al. 1995; Kurkdjian 1995). Ion selective vibrating probe studies have shown that both live bacterium *R. meliloti* as well as isolated Nod factors (NodRm-IV [S] can cause the membrane depolarization in alfalfa (*Medicago sativa*) root hair cells within 30-60 s after application. However, the fastest physiological response is an influx of calcium ion at the tip of the root hairs after about 15 second of addition of Nod factors (Allen et al. 1994, Felle et al. 1998). This is followed by consecutive transient and rapid increase in free Cl^- ion concentration (Felle et al. 1998) and a membrane depolarization (Ehrhardt et al. 1992: Felle et al. 1995; Kurdjian 1995). An increase of K^+ was also observed along with the depolarization event (Felle et al. 1998) Transient alkalinization of about 0.3 pH units was observed around the root hair zone along with depolarization. This increase in the extracellular pH was dependent on the concentration of applied Nod factors and parallel to the results obtained from intracellular pH increases due to different concentrations of Nod factor additions (Felle et al. 1996). Also an extracellular alkalinization has been observed in tomato suspension culture cells after treatment with Nod factors (Staehelin et al. 1994). Addition of a calcium ionophore A23187 ($Ca^{2+}/2H^+$ exchanger) mimicked the Nod factor response while the Ca^{2+} channel antagonist nifedipine inhibited the Nod factor response implicating the role of calcium as a secondary messenger in nod signal transduction (Lhuissier et al. 2001). The microtubule and actin cytoskeleleton play an important role in root hair growth. Changes of the actin cytoskeleton from the normal behavior, depolimerization of cytoskeletal parts, occur around 5 minutes after application of Nod

factors to the root hairs (Allen et al. 1994; Allen and Bennett, 1996; Cardenas et al. 1998; Miller et al. 1999; de Ruijter et al. 1999; Timmers et al. 1999).

2.2. Nematode parasitism

2.2.1. Economic importance

Plants and other organisms in the rhizosphere interact to form different associations that are either beneficial to both the plant and the organism or harmful only to the plant. One of these harmful interactions is between nematode and plants. Nematodes are a highly successful group of metazoans that inhabit most ecological environments. Some are free living and feed on microorganisms while others are parasitic on plants or animals (Williamson and Gleason, 2003). The success of nematodes is due to their inherent characteristics such as having a variety of feeding habits, a relatively short generation time, very high reproductive rates and a wide range of hosts (Trudgril and Blok, 2001). The nematodes interact with different parts of plants. For example, nematodes feed on almost all parts of the vascular plant including leaves, stems, flowers, seeds, bulbs and tubers and most of the roots (Bird and Kaloshian, 2003). One of the most harmful interactions is the pathogenic interaction between sedentary, obligatory, endoparasitic nematodes and roots of many plants. Cyst nematodes and RKNs are the most important groups forming this interaction causing crop losses in the billions of US dollars annually (Abad et al. 2003; Koenning et al. 1999; Sasser and Freckmann 1987).

The pathogenic interaction between RKN (*Meloidogyne spp.*) and many of their host plant species have greater economic importance since they interact with a wider variety of plants than cyst nematodes. The primary symptom of infection is induction of galls in the root

system, which greatly reduces the ability of the plant to take up water and nutrients. *Meloidogyne* species induce feeding sites in several thousands of plant species including crop plants such as potato, sugar-beet, soybean and tomato (Goverse et al. 2000; Jung and Wyss, 1999). They are wide spread in warm and hot climates.

Cyst nematodes mainly attack plants in temperate regions of the world. They are restricted to several families and among them the most important species has been recognized as *Heterodera* and *Globodera* (Jung and Wyss, 1999).

2.2.2. Nematode life cycle

Both cyst and RKNs have a generation time of about two months (Goverse et al. 2000). RKN, *M. incognita,* has a life cycle of about 4-6 weeks and *M. javanica* has a life cycle about 4 weeks (Tzortzakakis and Trudgill, 1996). Female nematodes lay thousands of eggs during their lifetime. For an example *M. javanica* produces about 2,000 eggs. The eggs are collected in a gelatinous matrix and secreted onto the root gall surface along a channel produced by the orifice of the female nematode (Orion and Frank, 1990). The hatched second stage juveniles (J2) enter the root at the elongation zone. Since they do not have a robust stylet as do cyst nematodes to cut the cell walls, they initially migrate to the root tip intercellularly between cortical cells and turn around to enter the vascular cylinder near the root tip and migrate up to the cell differentiation zone. The RKNs induce feeding sites in procambial cells, which undergo endoreduplication to form multinucleate giant cells (Williamson and Gleason, 2003, Jones and Payne, 1978). The J2 RKNs feed until the end of this growth stage and molt three times without feeding to become adult females. Most of the RKNs including

M. incognita reproduce by mitotic parthenogenesis to produce large number of eggs (Jung and Wyss, 1999, Trudgill and Block, 2001). The male RKNs only enter the plant during low nutrition conditions in a free living soil environment. Cyst nematodes enter the root by cutting the cell walls with their robust stylet and directly moving to the vascular cylinder. They initiate the permanent feeding site within the parenchyma cells in the vascular bundle. The cyst nematodes molt four times before maturity. Usually cyst nematodes reproduce sexually. Male cyst nematodes feed on the syncytia till the end of the J3 stage and become vermiform in J4. The adult males leave the root and mate with J4 stage females. These J4 females bear the fertile eggs and after their lifetime become the egg sac, which protects the eggs until they hatch (Jung and Wyss, 1999).

2.2.3. Induction of nematode feeding sites

Endoparasitic cyst and RKNs have the ability to change the developmental pathways of plants and redirect them to form specialized feeding structures. The mechanism that they use for these changes are unknown. Feeding sites induced by RKNs form giant cells while those induced by cyst nematodes form syncytia. Induction of RKN feeding structure is different from the cyst nematodes. RKNs initiate root knot galls with parenchyma cells, which are in close proximity to the nematode head in the vascular cylinder of the root. These cells increase their metabolic activity and cytoplasmic density similarly to syncytial cells. In these cells nuclear division occurs in the absence of cytokinesis to form several polyploid giant cells (Jones et al. 1981a).

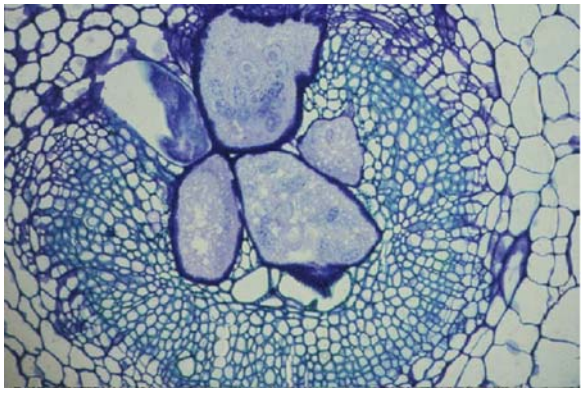

Figure 2.2 Transverse section of a *Meloidogyne incognita* induced root knot gall stained with toluidine blue to show large giant cells surrounded by cortical and pericycle gall or knot cells (Kindly provided by Dr. David McK. Bird).

The size of the fully developed giant cells is about 600-800 µm in length and 100-200 µm in width (Jones and Payne, 1978). 5-7 giant cells are induced by *Meloidogyne* species (Abad et al. 2003). A single giant cell has about 100 large nuclei with lobes. Nematodes feed from these giant cells using a "feeding tube" secreted from the stylet.

The feeding sites formed by cyst nematodes are called syncytia. The initial cells of syncytia, procambial parenchyma cells, in the vascular cylinder differ from other cells due to having increased metabolic activity, higher cytoplasmic density and lacking central vacuoles. The central vacuoles in these cells are reduced into small vacuoles. In addition, the syncytia are multinucleate and the nuclei are different since they become larger, amoeboid and multilobed. When the syncytium forms, the cell walls start to degrade around the pit area and gradually widen enough to fuse with the cytoplasm of the next cell. Likewise, the cell wall degrades forming a syncytia by joining the cytoplasm of about 200 neighboring cells along

the length of the vascular bundle becoming multinucleate feeding structures (Grundler et al. 1998**;** Jones et al. 1981a**).** The feeding tubes of cyst nematodes are probably used to filter and ingest the soluble food from the syncytia (Hussey and Mims, 1991).

2.3. Calcium and calmodulin in signal transduction

2.3.1. Calcium

Calcium acts as a secondary messenger in plants in response to many stimuli such as cold, touch and pathogens (Bush 1993). Different cellular organelles contain Ca^{2+} concentrations ranging from nanomolar to millimolar levels. In plant cell walls where calcium is used as a structural molecule, the Ca^{2+} concentration varies from 0.5 to 1 mM. In the vacuole and rough endoplasmic reticulum Ca^{2+} concentration is about 1 mM (Figure 2.3) (Trewavas, 2000). While cytosolic calcium concentration is low these intracellular calcium levels are tightly regulated in living cells to keep the resting cytosolic calcium concentration at 10^{-7} M (Trewavas, 2000).

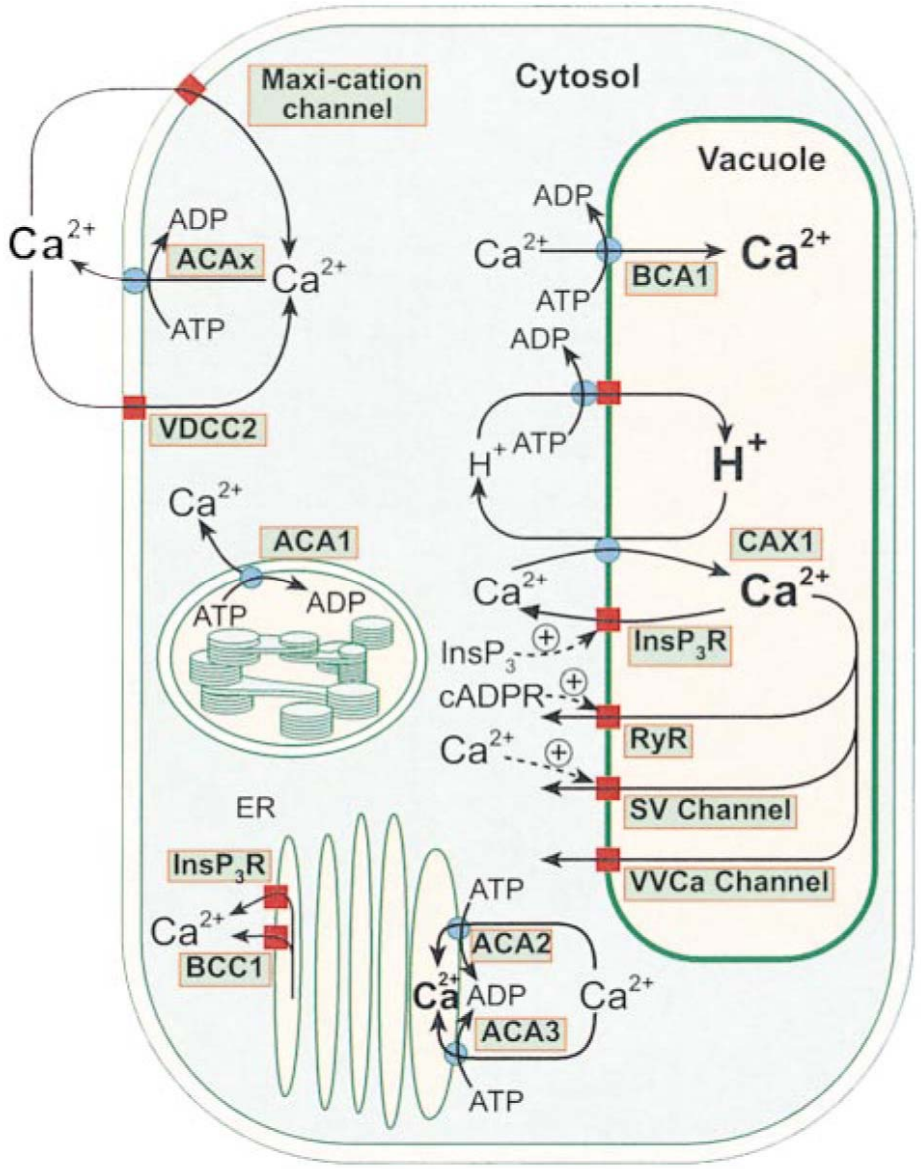

Figure 2.3 Schematic Representation of Major Identified Ca^{2+} Transport Pathways in Plant Cell Membranes. Modified from Sanders et al. (1999).

Calcium enters into the plant root cells through calcium permeable channels located in the plasma membrane (White, 2000). Once entered, it is sequestered in cellular organelles such

as the vacuole, endoplasmic reticulum, chloroplast and nucleus (White and Broadley, 2003). Different environmental stimuli can disturb the cytosolic calcium homeostasis. These perturbations are called "cytoplasmic calcium signatures" and are thought to be different from one stimulus to another by their magnitude, duration and cellular location (Bush, 1993; Berridge et al. 1998; Malho, 1999) (Figure 2.4). A high cytosolic calcium concentration is toxic to the cell. Therefore the calcium channels, transporters and pumps located in the plasma membrane and organelle membranes, carry out the regulation of changes of cytosolic calcium concentration in times of biotic or abiotic stress. The calcium pump, Ca^{2+}ATPase, present in the inner mitochondrial membrane, tonoplast and plasma membrane, together with the Ca^{2+}/H^{+} antiporters located in tonoplast and mitochondrial membranes remove the extra calcium from the cytosol to the stores in the cell wall and organelles (Sanders et al. 1999; Trewavas, 2000). The changes in cytosolic calcium levels are perceived by proteins such as, calmodulin, calcineurin B-like proteins and calcium dependent protein kinases (CDPKs) that are collectively called "cytoplasmic Ca^{2+} sensors". They can alter their catalytic activity or conformation when bound to the calcium and are able pass the signal downstream (White and Broadley, 2003).

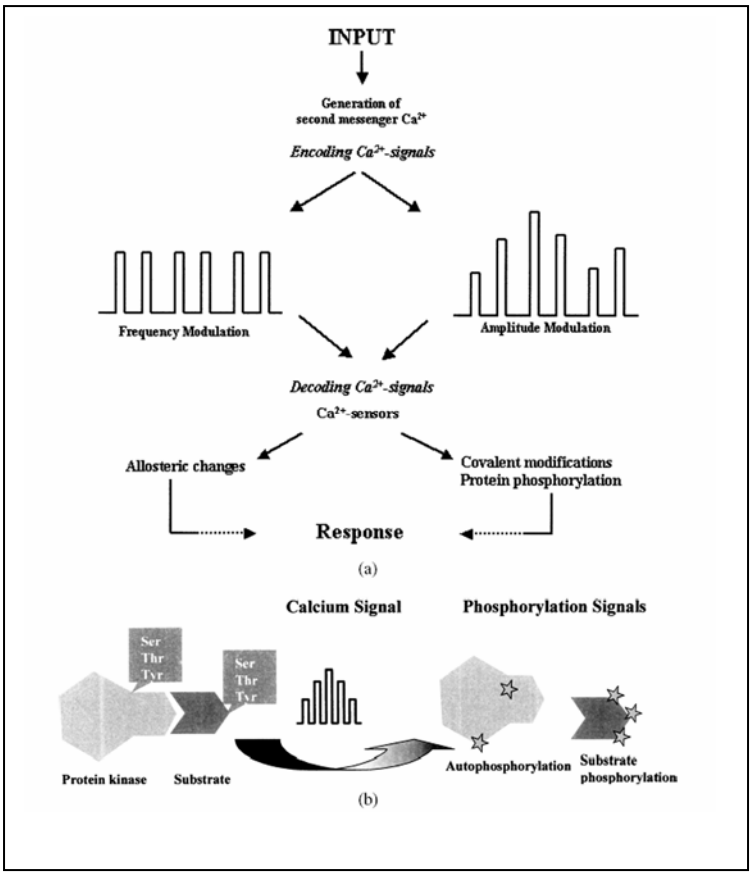

Figure 2.4 a) Encoding and decoding calcium signals, **b)** Decoding Ca^{2+} signals by protein kinases involve phosphorylation of the substrate and/or phosphorylation kinase. : Modified from Sathyanarayanan and Pooviah (2004) Critical Reviews in Plant Sciences.

2.3.2. Calmodulin

The primary calcium receptor in the plant cell is calmodulin (CaM), a ubiquitous protein found in both plants and animals (Zielinski, 1998). CaM is a highly conserved, highly acidic, dumbbell shaped, protein of about 16.7-16.8 kDa in size. It is located in cytoplasmic and nuclear compartments and can be attached to the plasma membrane in plant cells (White

and Broadley, 2003; Trewavas, 2000). CaM binds calcium with a high affinity using a helix-loop-helix structure called an "EF hand". Each of four EF hands on CaM is present in pairs, embedded in two globular domains within the molecule and binds to a single Ca^{2+} molecule (Zielinski, 1998).

The globular domain of CaM has a hydrophobic region that is rich in methionine, leusine, and phenylalanine. This region is closed in inactivated CaM. When calcium binds to the CaM, it undergoes conformational changes and hydrophobic patches open to the external medium. These hydrophobic regions can be identified by the calmodulin binding proteins and bind with the Ca^{2+}/ calmodulin complex activating the target proteins which activate the downstream signaling events (Zielinski, 1998; White and Broadley, 2003; Sathyanarayanan and Poovaiah, 2004).

2.3.3. CaM based calcium sensor cameleon and Fluorescence Resonance Energy Transfer

Cameleon is a calmodulin based calcium sensor that is composed of a calmodulin binding peptide M13 combined with either blue fluorescent protein (BFP) and green fluorescent protein (GFP) or cyan fluorescent protein (CFP) and yellow fluorescent protein (YFP) (Miyawaki et al. 1997). Calmodulin changes its conformation after binding to calcium and wraps around M13, which brings the two fluorescent proteins close enough together (20Å or more) to allow energy transfer between them. The FRET efficiency has been calculated to be inversely proportional to the sixth power of the separation distance between donor and acceptor proteins (Truong et al. 2001). When fluorescence resonance energy transfer occurs

the fluorescence of the donor protein, which gets excited by the external light source, will show reduced fluorescence intensity due to the transfer of the energy to the acceptor protein. The acceptor protein, however, which gets excited by the donor emission, increases its fluorescence emission intensity when CaM binds calcium. This method of energy transfer is widely used as a ratiometric imaging method and named fluorescence resonant energy transfer or FRET. FRET provides information about the closeness of the fluorophores that can be attached to the same molecule, as in the case of cameleons, or to different proteins to monitor their interaction (Zielinski, 1998). FRET is therefore an excellent technique to detect protein- protein interaction. Using cameleons as a calcium indicator has the advantage that it can be produced by the cells, avoiding the problems associated with introducing chemical calcium reporters into the cells. Furthermore it can be targeted into specific cellular compartments to monitor their calcium levels. However, it has to be kept in mind that the calcium signal obtained with cameleons is smaller than that obtained with chemical fluorophores and noise becomes a problem.

2.3.4. Calcium and Nod factor signal transduction

Calcium has been known to be involved in signaling in two different ways. One of the observations is that an increase of calcium occurs due to many different stimuli such as touch (Legue et al. 1997) cold (Knight and Knight, 2000) nodule formation. Munns (1970) showed that calcium is required for early stages of nodule formation in alfalfa (*M. sativa*). Allen et al. (1994) observed a calcium increase in alfalfa root hairs treated with Nod factor. Fura -2 or Fluo-3 loaded legume *Vigna unguiculata* root hairs showed a rapid plateau like increase in

intracellular calcium concentration within seconds after application of Nod factor (Gehring et al. 1997). The fastest reported response to Nod factor is an influx of calcium in alfalfa root hairs (Felle et al. 1998) after several seconds of Nod factor addition.

The second type of calcium signaling involves calcium spiking or cytoplasmic oscillations of calcium which is a wide spread phenomenon observed across animal (Berridge et al. 1998; 2003) and plant (Sathyanarayanan and Pooviah, 2004) kingdoms. The first reported calcium spiking in plants are from *Zea mays* coleoptiles and occurred due to IAA stimulation (Felle, 1988)**.** Calcium oscillations are also important for stomatal closure. The extracellular calcium induced cytoplasmic calcium oscillations of *de-itiolated 3* (*det*3) mutants of *Arabidopsis* recover their stomatal closure suggesting that cytoplasmic calcium oscillations are necessary for guard cell stomatal closure (Allen et al. 2000). Allen *et al* (2001) showed that short term stomatal closure is due to elevation of cytoplasmic calcium levels and steady state stomatal closure are due to cytoplasmic calcium oscillations.

The dextran linked calcium sensitive dye, calcium green, injected into alfalfa root hairs were used to observe the changes of cytoplasmic calcium treated with Nod factors by Ehrhardt et al. (1996). Localized periodic calcium spiking occurred after about nine minutes of Nod factor application with a sixty second mean difference of time in between spikes and continuing for about an hour. Non-nodulating mutants of alfalfa (MN-NN1008) that do not show cortical cell division root hair deformations, lack the calcium spiking, implying that the mutants are blocked in early signal perception and calcium spiking is necessary for the nodulation process to occur. Calcium spiking has been observed in several other legume root hairs such as *L. japonicus* (Harris et al. 2003), *Pisum sativum* (Walker et al. 2000) and

M. truncatula (Wais et al. 2000*)* and is the only Nod factor induced response that is commonly observed in several legume genera and species. Nod factor calcium changes depend on concentration. In *M. truncatula* root hairs, two different calcium responses were observed with 1 nM and 10 nM Nod factor concentrations. With 1 nM Nod factor, the usual calcium spiking was observed and with 10 nM Nod factor an immediate temporary increase of calcium levels was seen followed after 10 min of calcium spiking. This result indicates a potential branching point in the early signal transduction pathway (Shaw and Long, 2003).

3. MATERIAL AND METHODS

3.1. Plant preparation

3.1.1. Plant material

L. japonicus ecotype Gifu, Nod factor receptor mutants *nfr1*, *nfr5* and symbiosis receptor-like kinase mutant *symRK* were grown at 22^0C in a growth chamber under 16 hr light and 8 hr dark cycle. The seeds were collected when the outside of the seed pod became brown.

3.1.2. Germination of seeds

Lotus seeds were scarified and sterilized in concentrated sulfuric acid for 5-10 min and washed with sterile water 5-6 times to remove the acid. Seeds were then placed on a sterile stack of 3 moist filter papers, wrapped with plastic and aluminum wrap and germinated in the dark for 2-3 days.

3.1.3. Transformation of *Agrobacterium rhizogenes* with pBinHYC6.1

The construct pBinHYC6.1 (Figure. 1) (kindly provided by Dr. John Love, UK and with permission from Dr. Mitsuhiko Ikura) was electroporated into *Agrobacterium rhizogenes* strain AR10. The cells were grown on LB (Lauria Bertani) with 50 μg/μl of kanamycin and 300 μg/μl rifampicin (1.2% Agar). The presence of the plasmid in individual colonies was checked by DNA gel electrophoresis (Figure 3.2).

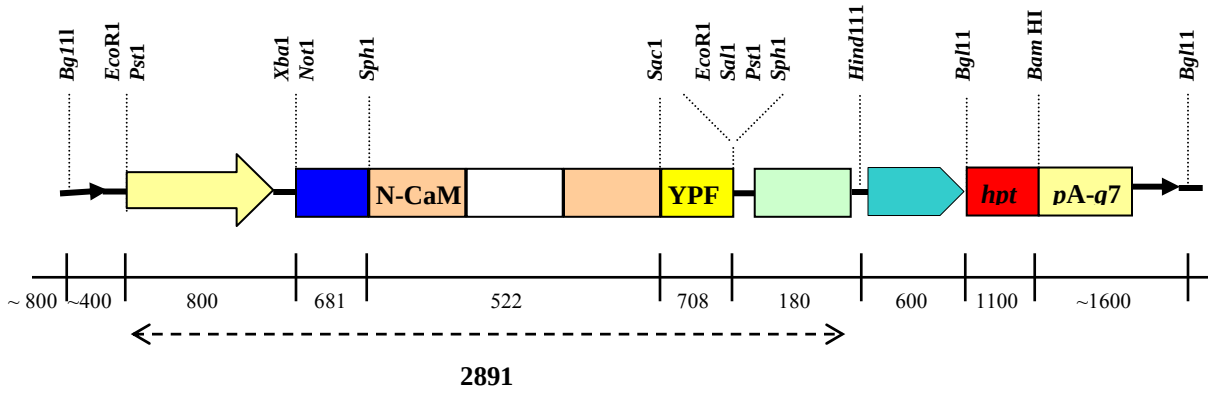

pBinH-YC6.1

Figure 3.1 Map of the cameleon puc18 based construct, which confers resistance to kanamycin in bacteria and hygromycin in plants. It also expresses both GFP and YFP and this cameleon can be used to measure Ca^{2+} concentration in cells.

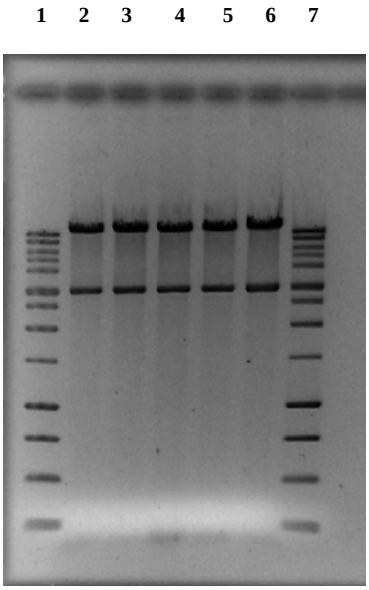

Figure 3.2 Plasmids were isolated from *A. rhizogenes* colonies (column 2-6), cut with *Hind*111 and *Eco*R1 and run on an agarose gel. Column 1 and 7 show the 1 kb ladder.

3.1.4. Transformation of *Lotus japonicus*

Lotus japonicus plants were transformed according to Stiller *et al* (1997). *A. rhizogenes* were grown on LB/Agar/Rifampicin/Kanamycin and the bacteria were harvested using a sterile spatula and suspended in 1 ml of sterile water. 2-3 day old seedlings were grown on half strength Gamborg's B5 medium with 1.2% agar and were inoculated with bacteria suspended in sterile water. B-D syringes (1 ml 26G Turberculine slip tip, Bectin Dickinson & Company, New Jersey) were used to wound the hypocotyl area just below the cotyledons of the seedlings and 1-2 drops of *A. rhizogenes* suspension was placed on the wound. Inoculated plants were kept in the dark at 22 ^{0}C overnight. The plants were uncovered and kept at 22 ^{0}C with a 16hr light/8hr dark cycle until hairy roots were generated. Plants with hairy roots were transplanted on to cover slips (# 0, 24 x 64 mm), embedded in 1.2% Agar prepared with half strength Gamborg's media with 300µg/ml cefotaxime and grown at 22 ^{0}C with a 16 hr light 8 hr dark cycle for 2-3 weeks until the hairy roots were long enough to use for the experiments (Figure 3.3).

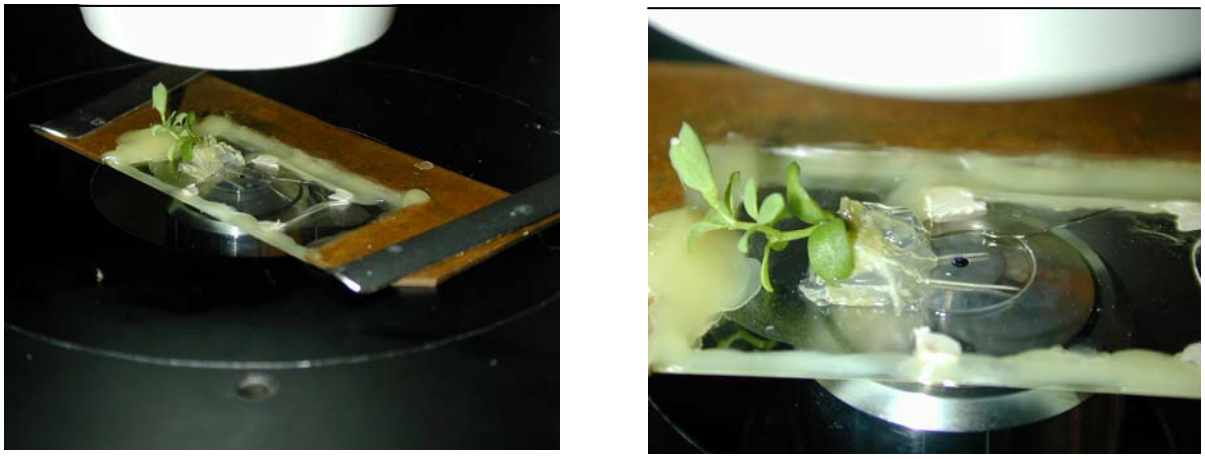

Figure 3.3 *L. japonicus* plant with hairy roots grown into the embedded agar on a cover slip (#0, 24x 64 mm). These images also show the perfusion chamber in which experiments were performed.

Lotus roots were incubated for 5, 10, 15, and 30 min in 4 μM Fluo-4 acetoxymethyl ester prepared in 0.5X Gamborg's B5 medium. These roots were imaged using a Leica (DM IRDB SP1) confocal laser scanning microscope with 40x oil objectives using an excitation wavelength of 488nm and emission wavelength of 516 nm.

3.1.5. Indo-1 loading

Two-day old seedlings were transplanted to a #0 cover slip attached to the bottom of a drilled glass slide and covered with a thin layer of 0.8% low gelling temperature agarose (Agarose VII, Sigma) (Figure 3.4). Slides were slanted at a 45^0 angle in culture boxes that were filled with Gamborg's B5 medium up to the level of the cover slip and kept for two days in a 22 ^{0}C growth chamber.

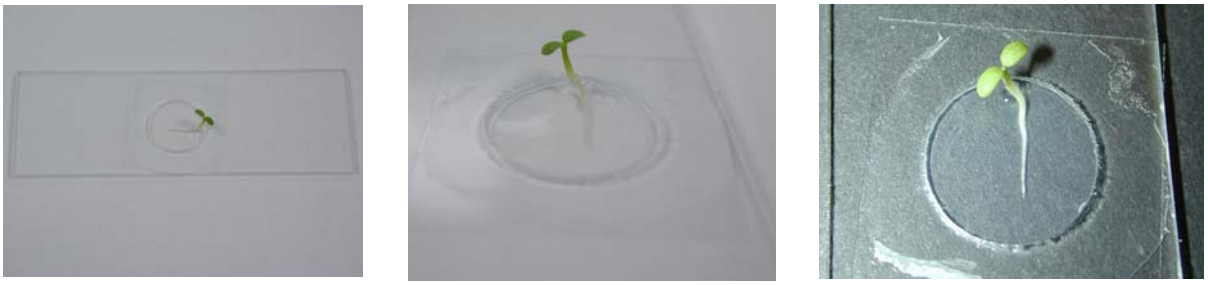

Figure 3.4 *Lotus japonicus* plants growing on a cover slip. This set- up was used when imaging Indo-1 loaded plants.

Roots were washed several times with 0.5x Gamborg's B5 medium supplemented with 15 mM MES adjusted to pH 4.5 with KOH. Roots were then covered with 150 µL of 50 µM Indo-1 (pentapotassium salt *cell impermeant*) [Figure 3.5 & 3.6] {Invitrogen Corporation, 1600, Faraday Avenue, Carlsbad, CA} dissolved in the same media in which roots were washed. The seedlings were kept at a slant for 1 hr with the roots covered so no light was received. Indo-1 was removed and the plant was washed with 0.5X Gamborg's medium 5-6 times before imaging.

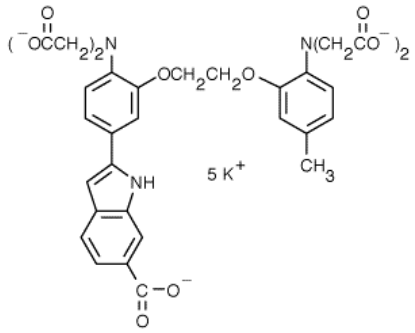

Figure 3.5 1H-Indole-6-carboxylic acid, 2-[4-[bis-(carboxymethyl)amino]-3-[2-[2- (bis-carboxymethyl) amino-5- methylphenoxy]ethoxy] phenyl]-, pentapotassium salt (http://www.invitrogen.com, Invitrogen corporation).

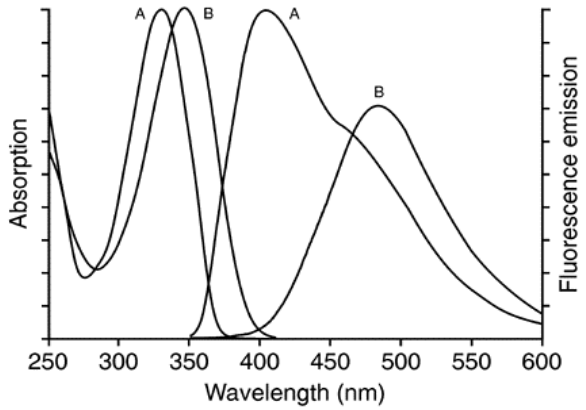

Figure 3.6 Absorption and fluorescence emission (excited at 338 nm) spectra of Ca^{2+}-saturated (A) and Ca^{2+}-free (B) indo-1 in pH 7.2 buffer (http://www.invitrogen.com, Invitrogen Corporation].

3.2. Treatments

3.2.1. Calibration of the free calcium

A Calcium calibration buffer kit with magnesium #2 (Molecular Probes, Eugene, OR) was used to calibrate the free calcium in the cytoplasm. External calibration was done with 50 µm Indo-1 and eleven buffers with different free calcium concentrations (0.00, 0.017, 0.038, 0.065, 0.100, 0.150, 0.225, 0.351, 0.602, 1.35 and 39 µM).

3.2.2. Nematode preparation

Nematodes (*M. incognita*) that were grown on tomato plants (Lohar et al. 2004) were used to collect the egg masses as described in Hussey and Barker (1973). Eggs were collected after

shaking the roots with 1% NaOCl on to a 25 µm sieve. Eggs were cleaned on a sucrose (40%) gradient and washed on a 25 µm sieve and placed on moist tissue paper to hatch. Secondary stage larvae (J2) that migrated through the tissue paper were collected and surface sterilized with 1% NaOCl and suspended in 0.5X Gamborg's B5 medium.

3.2.3. Ionophore treatment

150 µM Calcium ionophore A23187 (Sigma-Aldrich, Saint Louis, Missouri) was dissolved in DMSO and added to the Indo-I loaded roots and the hairy roots transformed with the cameleon.

3.2.4. Mastoparan-7 treatment

200 µl of 7.5 µM mastoparan-7 (Mas-7) dissolved in 0.5X Gamborg's B5 medium was perfused into the roots that were loaded with Indo-1.

3.3. Imaging

3.3.1. Microscopy

Ratio imaging of the cameleon GFP transformed plants was performed with a Zeiss Axiovert 100 TV inverted microscope using a 40X (NA=1.25) Neofluar oil immersion objective [Carl Zeiss Thornwood, NY]. Seedlings were mounted on #0 cover slips attached to a metal holder and a perfusion chamber was constructed using polymer clay and Valap to allow for introduction of nematodes and chemicals during data acquisition. A dual emission filter set

cameleon 2 (Figure. 5) [Chroma Technology Corp, San Diego, CA] with D440/20 nm excitation filter, 455DCLP dichroic beam splitter, D485/40 nm emission filter for cyan, D535/30 nm emission filter for yellow was used for illumination of the cameleon expressing plants. Illumination was performed using excitation and emission filters controlled by Lambda 10-2 controller [Sutter Instruments, 51, Digital Drive, Novato, CA] and Metafluor software [Universal Imaging, West Chester, PA]. A cooled CCD camera [ORCA-ER, Hamamatsu, Hamamatsu City, Japan] was used to collect fluorescence images at the two emission wavelength and DIC images at 3, 5 or 30 s intervals as indicated. The fluorescence intensity for images taken at each of the two emission wavelengths was determined for selected cytoplasmic areas that were followed frame by frame using Metafluor software. The ratio (emission intensity from 520-550 nm over emission intensity from 465-505 nm) was then plotted over time using excel software (Microsoft Corporation, Redmond, WA).

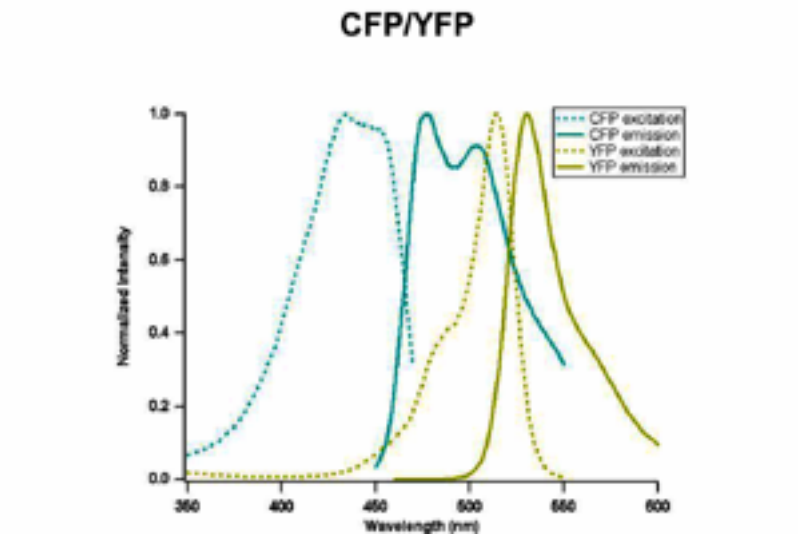

Figure 3.7 Spectra of CFP and YFP. From www.embl.org (European Molecular Biology Laboratory, Heidelberg, Germany).

3.3.2. Confocal microscopy

Indo-1 loaded root hairs of 2-day old *L. japonicus* seedlings were imaged using a Leica SP1 laser scanning confocal system (Leica, Deerfield, IL) attached to a Leica DM IRDB inverted microscope. Indo-1 loaded root hairs were imaged with a 40X (NA=1.2) oil immersion objective. The sample was excited using a UV laser (351 nm) and emission was collected from 400-445 nm (E1) and 460-500 nm (E2) with photo multiplier tubes. Differential Interference Contrast (DIC) images were recorded simultaneously with the transmitted light detector. Images were collected in intervals of 3 and 30 s. Fluorescence intensities of selected cytoplasmic regions were measured with the Leica confocal software (Version 2.5) [Leica Microsystems, Heidelberg, Germany] and Metafluor software. The ratio (E1/E2) was plotted over time using Excel 2000.

4. RESULTS

4.1. Cameleon-expressing plants did not report cytosolic Ca^{2+} changes after treatment with calcium ionophore A23187, Nod factors, touch or RKN.

The cameleon construct pBinH-CY6.1 was successfully expressed in the cytoplasm of wild type *L. japonicus* (Figure 4.1) *L. japonicus* mutants s*ym*RK and *nfr-1*. The cameleon expressing root hairs were excited at 440/20 nm and emission was collected at 465-505 nm and 520-540 nm. The regions were marked and the fluorescence intensity ratio (emission intensity from 465-505 nm over emission intensity from 520-540 nm) was plotted as a function of time.

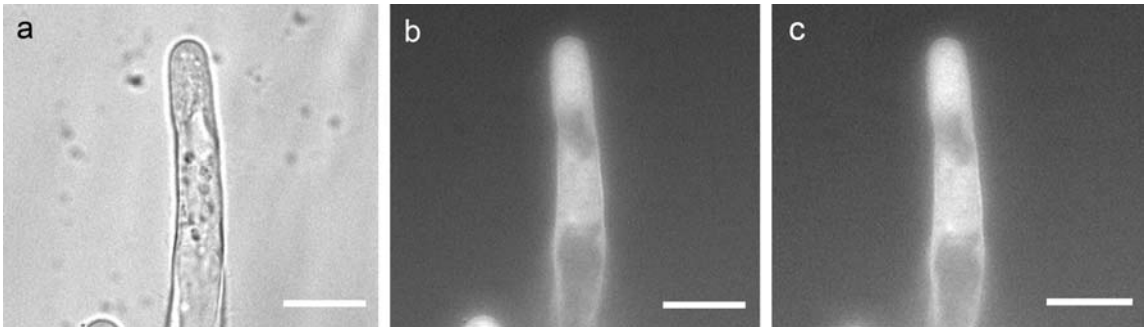

Figure 4.1 Cameleon expressing root hairs of *Lotus japonicus.* **a)** DIC image of wild type *Lotus japonicus.* **b)** fluorescence image from channel one (465-505 nm) and **c)** fluorescence image from channel two (520-550 nm). The image collected at 520-550 nm had a higher intensity. The intensity ratio did not change after addition of calcium ionophore A23187, nod factors or touch stimulation.

4.2. Imaging of *Lotus Japonicus* root hairs

4.2.1. Indo-1 is a cytoplasmic calcium indicator

Since the cameleon did not allow for the collection of calcium concentration change data, I tried different calcium indicator dyes hoping that one would remain in the cytoplasm long enough to carry out imaging over time. Fluo 4 went into the vacuoles within five min. However Indo-1 stayed in the cytoplasm and was chosen for the following experiments. Indo-1 is a chemical fluorescent probe that is widely used as a calcium indicator in both animal and plant cells. It has a dissociation constant (K_d) of 230 nM *in vitro* conditions (at pH 7.2 and 25 ^{0}C) (http://probes.invitrogen.com/handbook/tables/0370.html). In addition, it has two emission maxima at (410 nm) and at (485 nm) (Figure 4.2). After calcium ions bind the indo-1, it undergoes a spectral shift changing the intensities of the two wavelength ranges shown above increasing the emission at 400-445 nm and lowering the emission at 460-500 nm (Figure 4.2). Normally, Indo-1 is acid loaded into the cells using strong acids buffered at pH 4.5. Around pH 4.5 the Indo-1 becomes fairly neutral having 50 % of the protons dissociated. At this point Indo-1 becomes lipophilic and diffuses through the plasma membrane. Since the cytoplasmic pH (~7.00) is much higher than the loading value (pH 4.5), Indo-1 loses its proton becoming an ionic form. This ionic form cannot penetrate the membrane and therefore stays in the cytoplasm. The images clearly show no fluorescence in vacuoles, the indo-1 stays only in the cytoplasm.

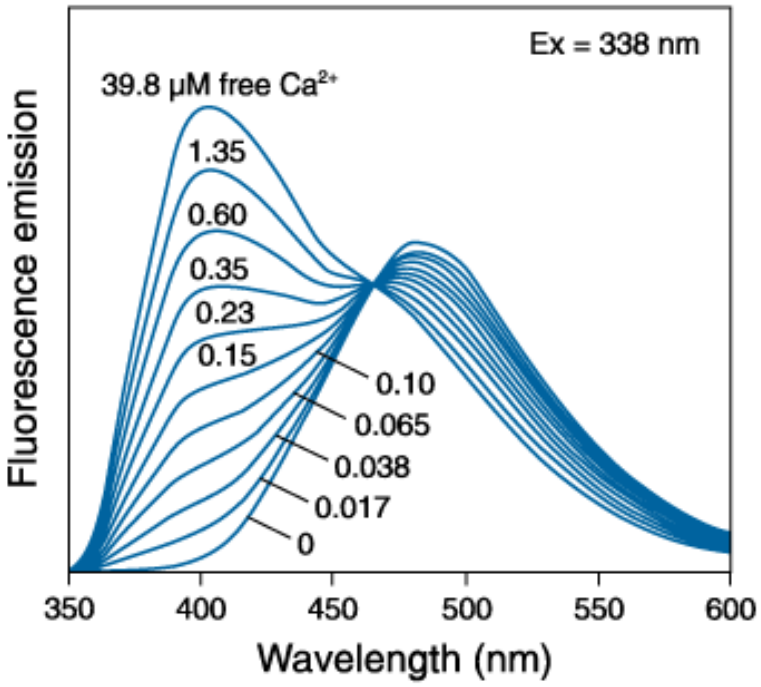

Figure 4.2 Spectrum of Indo-1 responding to 351 nm excitation at various [Ca^{2+}].

4.2.2. No auto fluorescence detected in *L. japonicus* root hairs

Different organelles in the cells might show auto fluorescence when excited with ultraviolet (UV) radiation (Takahashi et al. 1999). The fluorescent dye Indo-1 was used in this study as an indicator for cytoplasmic calcium and excites in the UV wavelength (351 nm) and emits in the range of 400-445 nm and 460-500 nm. To determine if root hairs of *L. japonicus* have auto fluorescence in the UV wavelength range these roots were imaged at these wavelengths. Root hairs, not loaded with Indo-1, had hardly any auto fluorescence in conditions used in

the following experiments (Figure 4.3.), therefore, the signal intensity observed in root hairs was considered directly proportional to the indicator emissions in this entire study.

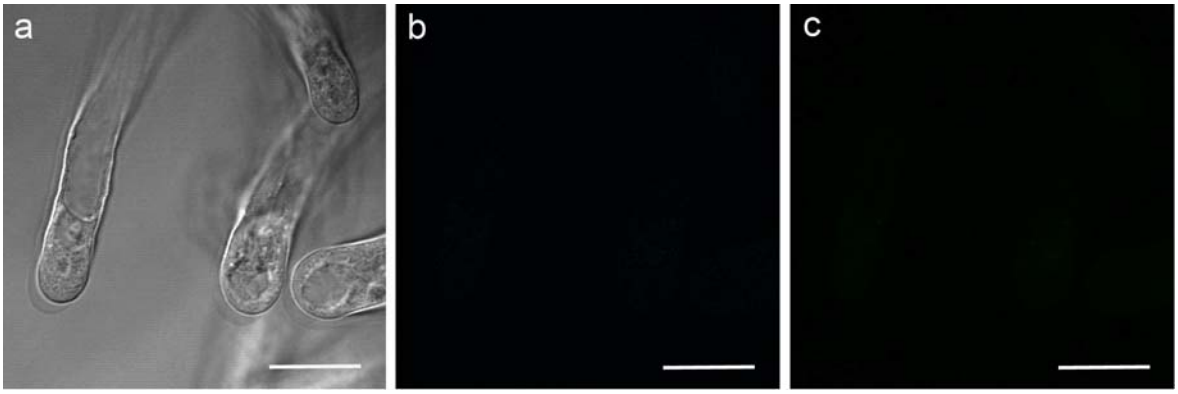

Figure 4.3 *L. japonicus* root hairs imaged to visualize the presence of autofluorescence under excitation of UV at 351 nm. Images were recorded simultaneously in **a)** DIC, **b)** channel 1(400-445 nm) and **c)** channel 2 (460-500 nm). Scale bar 10µm**.**

4.2.3. Growth and behavior of Indo-1 loaded root hair cells

Root hairs were acid loaded with 50 µM Indo-1 at pH - 4.5, 2-(N-morpholino) ethanesulphonic acid (MES) and their normal growth was observed for 1 hr on a confocal microscope with an excitation 351 nm and emission windows of 400-445 nm and 460-500 nm (Figure 4.4b and 4.4c). Figure 4.3 illustrates a root hair that was loaded with 50 µM Indo-1 for 1 hour, washed 5 times with pH = 7.2 medium to remove the residual dye and imaged on a confocal microscope using excitation at 351 nm. Their growth and streaming behaviors were recorded. Figure 4.3a depicts the differential interference contrast (DIC) image simultaneously recorded with fluorescent images (Figure 4.4b & 4.3c) taken at a range

of 400-445 nm (channels-1) and 460-500 nm (channels-2). Growth rates and cytoplasmic streaming were identical to that seen in the root hairs that were not loaded with Indo-1.

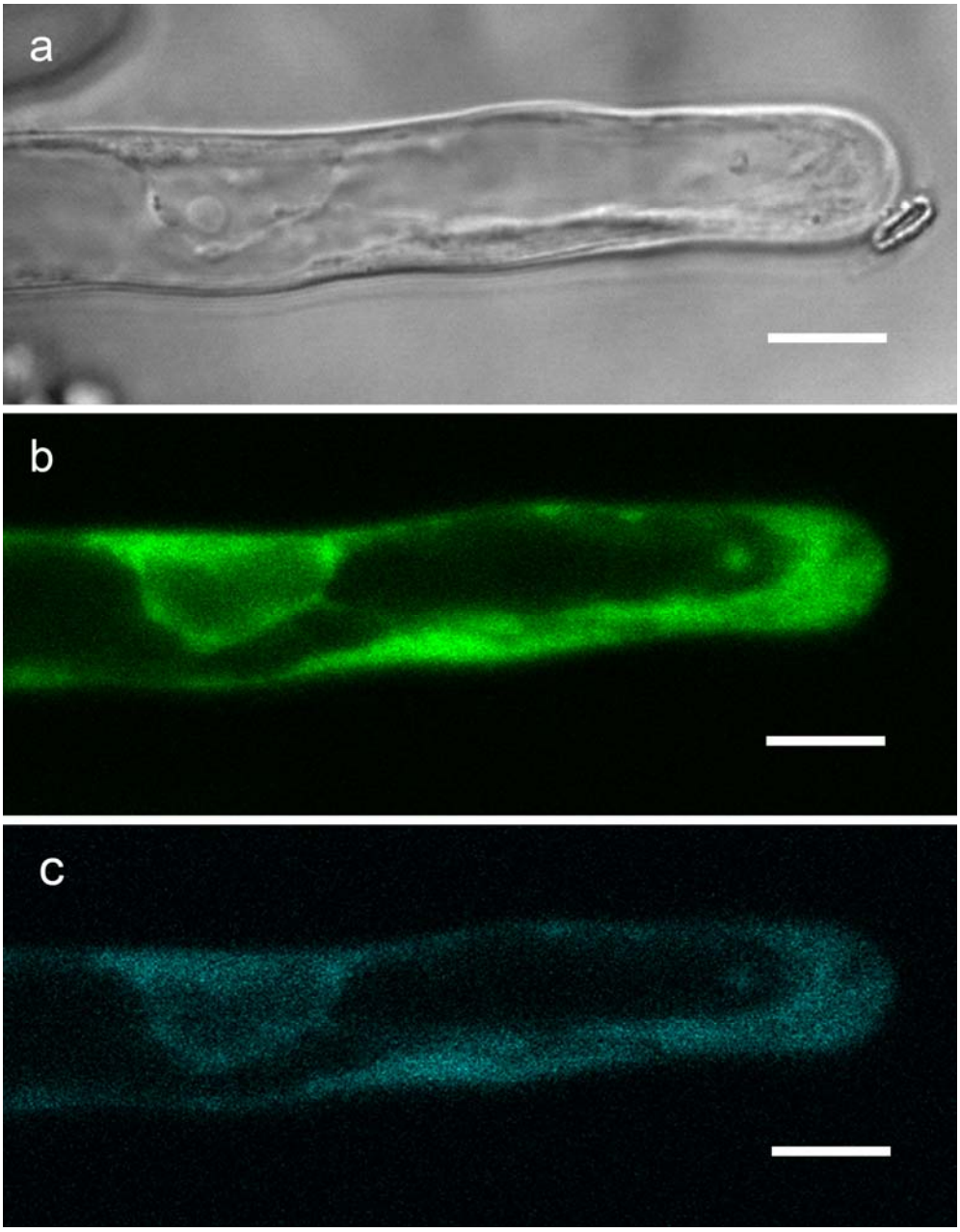

Figure 4.4 A *L. japonicus* root hair loaded with 50 µM Indo-1 for 1 hr and washed 5 times with medium to remove the residual dye. The dye is clearly fluorescing. The differential interference contrast (DIC) image **a**) simultaneously recorded with fluorescent images, **b and c)** taken at a range of 445-450 nm (channels-1) and 460-500 nm (channels-2) on a confocal microscope. Scale bar is 10 µm.

4.2.4. Ratio imaging

Ratio imaging was performed with the ratiometric dye Indo-1 using confocal laser scanning microscopy. The emission intensities collected in the wavelength range 400-445 nm were divided by the emission intensities collected at 460-500 nm to obtain the intensity ratio, which is used to calculate the cytoplasmic calcium concentration. Ratio imaging is insensitive to uneven dye loading, photo bleaching and thickness of the specimen (optical path length). Since Indo-1 has two emission rather than two excitation wavelengths, fluorescence images can be recorded at the same time using two different photomultipliers as detectors.

4.3. Data analysis

4.3.1. Ratio data was transferred to UI Metafluor software for analysis of calcium concentrations

Several root hairs were seen in each fluorescent image and cytoplasmic regions to be measured were marked on the image (Figure 4.5c). The intensity data obtained from marked region was logged into an Excel sheet. Due to cytoplasmic streaming and organelle movements, the locations of the marked areas could change over time and therefore, the regions had to be redone and data had to be logged for each new frame. In this study, we focused only on two cytoplasmic regions, one at the root hair tip and the second at cytoplasmic areas surrounding the nucleus. These two areas are the regions in which calcium changes have been observed in response to Nod factors. The intensity ratios of these regions were plotted against time using KaleidaGraph software (Synergy Software, Reading, PA).

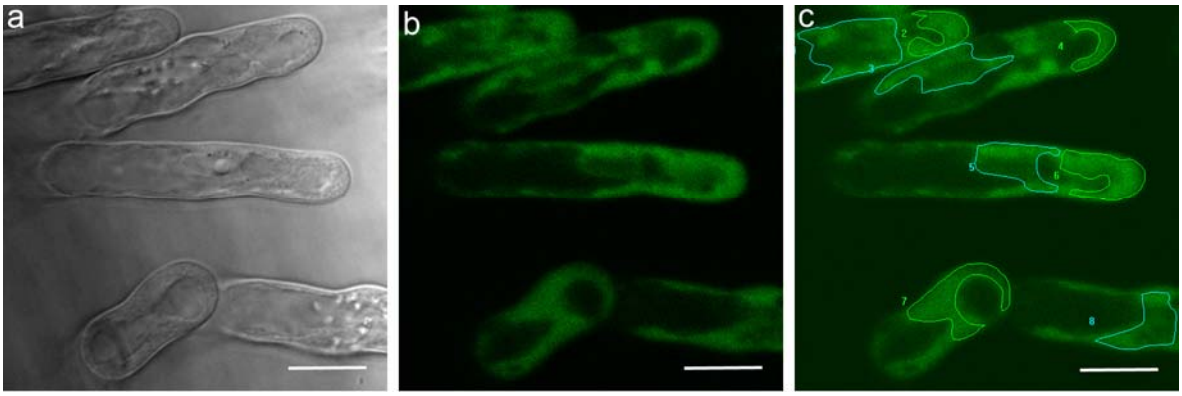

Figure 4.5 Regions of cytoplasm selected with Universal Imaging Metafluor software for intensity measurements. **a)** DIC image with five different root hairs showing cytoplasmic regions, **b)** Indo-1 loaded UV excited root hairs showing fluorescence in the cytoplasm, **c)** marked regions of image b. Scale bar is 10 μm.

4.3.2. Analysis of data using the Leica confocal software package to obtain the ratio intensities used when cytoplasmic areas were stable.

Leica confocal software was used to analyze the data from *in vitro* calibrations on the occasions when there was no movement. Mostly the analysis was done as indicated above using the UI software. Tip and nuclear regions were marked as described in (4.3.1) and the data was transferred to Excel from which intensity ratios could be calculated.

4.4. How valid are the cytoplasmic calcium measurements using Indo-1?

4.4.1. *In- vitro* calibrations of free calcium

Ratios are a reflection of the changes in cytoplasmic calcium concentration. In section 4.4.2 it is shown that *in vivo* calibrations were not possible because the calcium ionophores did not

give an immediate calcium response. In order to know the actual calcium concentration, *in vitro* calibrations were performed using the "Calcium Calibration Buffer kit with Mg^{2+} # 1" from Molecular Probes.

The intensity ratios obtained from eleven different free calcium buffers with 50 μM Indo-1 are shown in Table 4.1. Calibration curves obtained from the *in vitro* calibration with Indo-1 showed a quite linear relationship at low calcium concentrations (Figure 4.6). The calibration curve is nonlinear at higher calcium concentrations even though drawn as linear in figure 4.6. Therefore it cannot be used to obtain corresponding calcium concentration for the intensity ratios.

Table 4.1 Intensity values obtained with different free calcium concentrations.

Free Ca^{2+} Concentration	Mean Intensity of Channel - 1	Mean intensity of Channel - 2	Intensity Ratio [Channel-1/channel 2
0.000	37.07	130.56	0.28393
0.017	27.04	85.58	0.315961
0.038	27.89	86.04	0.324151
0.065	26.75	78.81	0.339423
0.100	68.81	191.51	0.359302
0.150	59.24	147.26	0.402281
0.225	70.27	156.90	0.447864
0.351	58.84	116.46	0.505237
0.602	61.78	101.10	0.611078
1.350	62.88	77.45	0.811878
39.00	82.35	77.16	1.067262

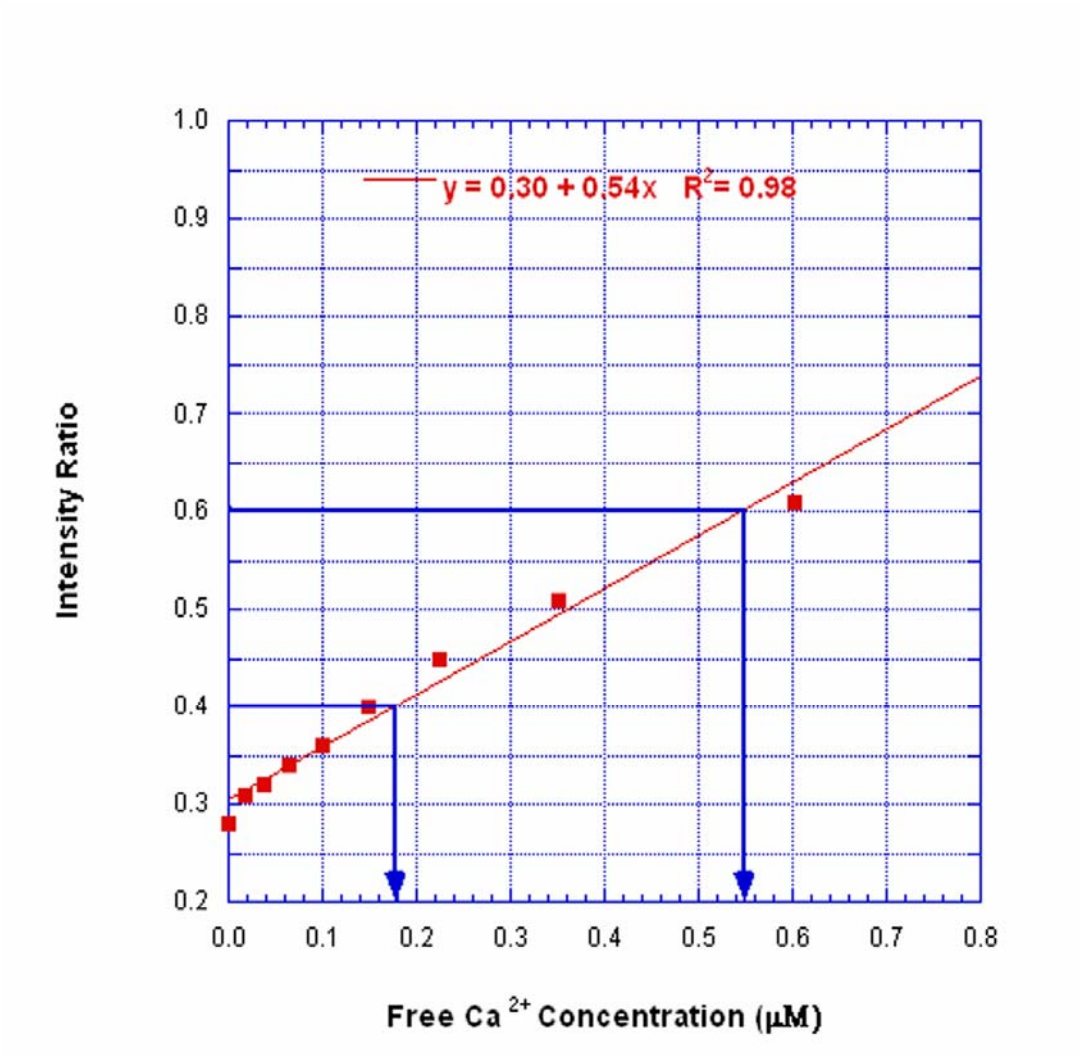

Figure 4.6 Intensity ratios plotted as a function of the free calcium concentration. The blue arrow shows that at a ratio value of 0.4, the calcium concentration is 0.18 µM or 180 nM. For intensity ratios of 0.6, the [Ca^{2+}] is 550 nM.

4.4.2. Effect of the calcium ionophore A23187 on cytoplasmic calcium levels

The calcium ionophore, A23187, was used to observe the calcium changes in Indo-1 loaded cells. One would expect that it would permeabilize the plasma membrane and raise calcium ion levels in the cytoplasm quite quickly. After imaging for 5 min, the ionophore was perfused into the chamber while imaging of the root hairs was continued (Figure 4.7). The expected sudden rise (Felle et al. 1998) of cytoplasmic calcium levels was not observed. But compared to the control (Figure 4.9), there was a significant increase of about 240 nM (P = 0.001) in the cytoplasmic calcium level in response to A23187.

Table 4.2 Effect of the calcium ionophore treatments on root hairs.

Root hair number	Ratio change for 0-5 min measurements	Ratio change for 25 - 30 min measurements	A234187 Intensity ratio change
1	0.5837 ± 0.010	0.7420 ± 0.01	0.160
2	0.7200 ± 0.009	0.7776 ± 0.03	0.057
3	0.5999 ± 0.015	0.7101± 0.04	0.120
4	0.8661± 0.030	1.0280 ± 0.04	0.160
5	0.7680 ± 0.020	0.9205 ± 0.02	0.150
Mean change in intensity ratio			**0.130 ± 0.04**

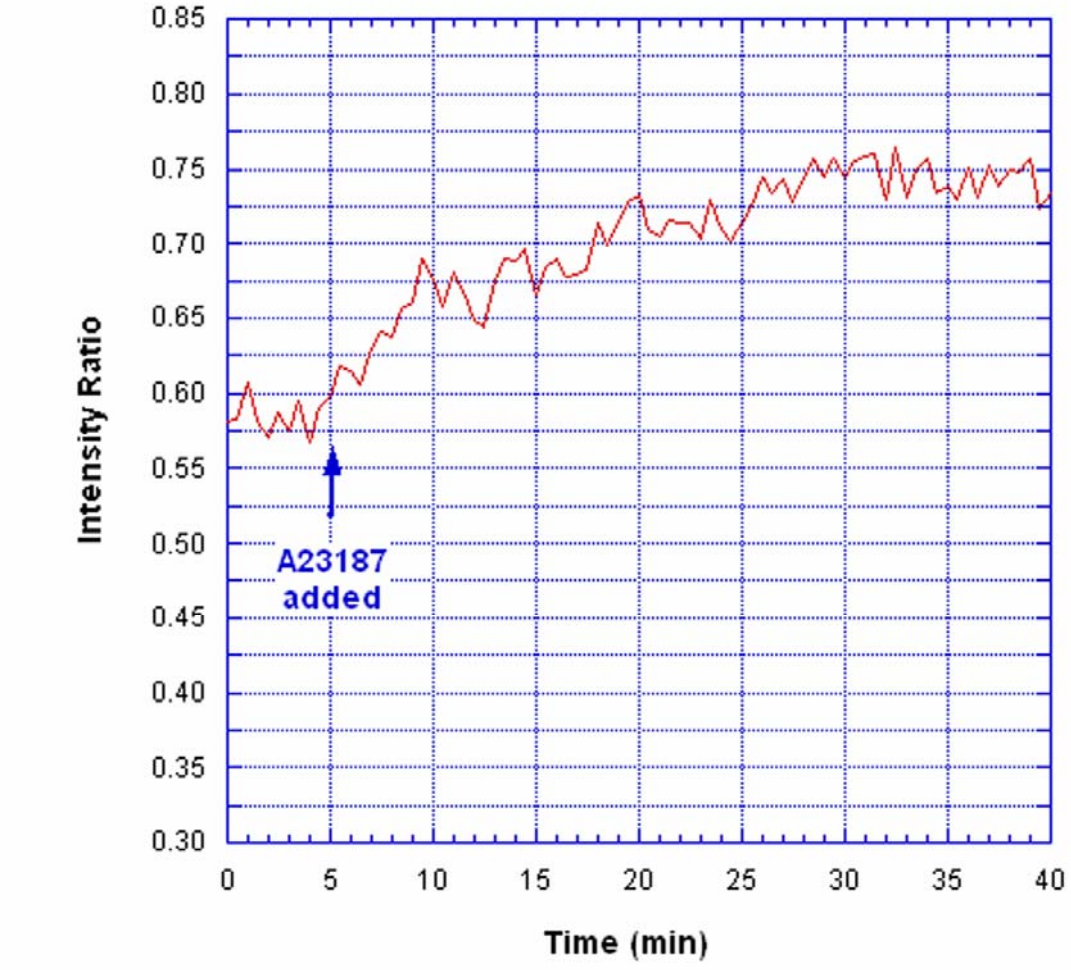

Figure 4.7 Cytoplasmic calcium increases 0.130 intensity ratio units gradually after A23187 addition.

4.4.3. Effect of Mas-7 treatment on cytoplasmic calcium levels

The root hairs of *L. japonicus* were treated with the mastoparan analogue, Mas-7. Images were collected every 30 s. Mas -7 was perfused after 5 min and imaging continued for 30 min (Table 4.3). The data are presented in Figure 4.8. Mas-7 permeabilizes the plasma membrane so that calcium ion can go through and enter the cytoplasm. So a sudden increase of intracellular calcium concentration should result. However, compared to the control, (Figure 4.9) no significant increase of cytoplasmic calcium levels were observed in Mas-7 treated root hairs ($P = 0.47495$).

Table 4.3 Summary of data obtained from addition of Mas-7 to *L. japonicus* root hairs.

Root hair number	Ratio change for 0-1 min measurements	Ratio change for 16.5-21.5 min measurements	Intensity ratio change
1	0.7489 ± 0.020	0.7657 ± 0.01	0.016
2	0.7625 ± 0.020	0.7569 ± 0.01	-0.005
3	0.7247 ± 0.009	0.7542 ± 0.01	0.029
4	0.6899 ± 0.010	0.7485 ± 0.02	0.058
5	0.6491 ± 0.040	0.6634 ± 0. 01	0.014
Mean change in intensity ratio			**0.022 ± 0.005**

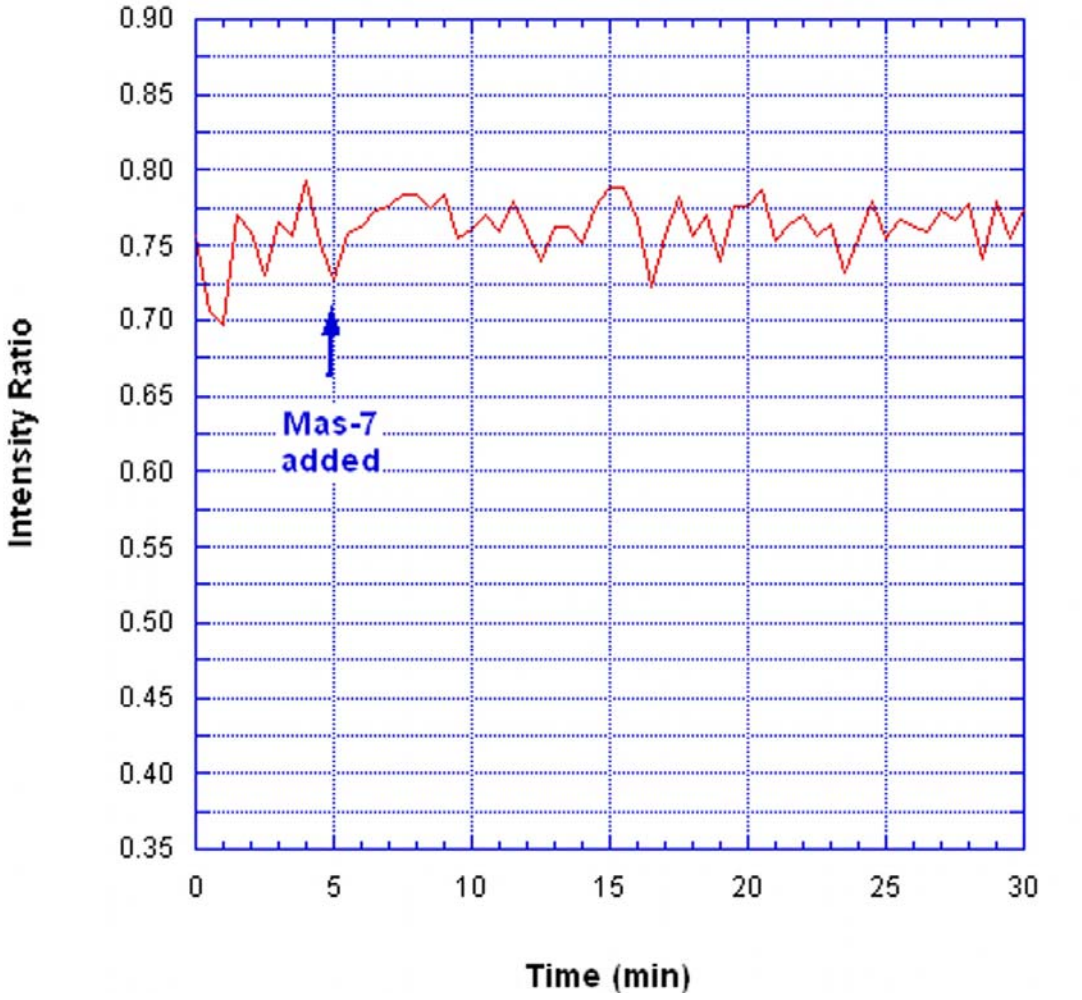

Figure 4.8 No change of cytoplasmic calcium levels was detected after addition of Mas-7 to *L. japonicus* root hairs.

4.5. Changes in cytoplasmic calcium levels in root hairs due to Nod factor and nematode treatments

4.5.1. No changes in cytoplasmic calcium levels were seen after only the Gamborg's medium was perfused over *L. japonicus* root hairs

Three different protocols were employed to capture calcium change at different time points. This was necessary because of photobleaching problem. Nod factors and RKNs were suspended in Gamborg's medium. In order to test the possible effect of this medium, indo -1 loaded *L. japonicus* root hairs were perfused with it. Indo-1 intensity was imaged for 5 min and then the roots were perfused with Gamborg's B5 medium (Table 4.4) and imaged for another 25 min. The Gamborg's media did cause an insignificant change in the mean intensity of 0.021 at the tip of root hairs (Figure 4.9).

Table 4.4 Summary of data recorded from the addition of Gamborg's media as a control for RKN additions.

Root hair number	Ratio change for 0-5 min measurements	Ratio change for 25-30 min measurements	Intensity ratio change
1	0.7056 ± 0.010	0.7110 ± 0.010	0.005
2	1.0956 ± 0.007	1.1406 ± 0.010	0.044
3	0.4977 ± 0.008	0.5126 ± 0.010	0.014
4	0.5575 ± 0.020	0.5791 ± 0.007	0.022
5	0.4418 ± 0.012	0.4758 ± 0.009	0.023
Mean change in intensity ratio			**0.021 ± 0.01**

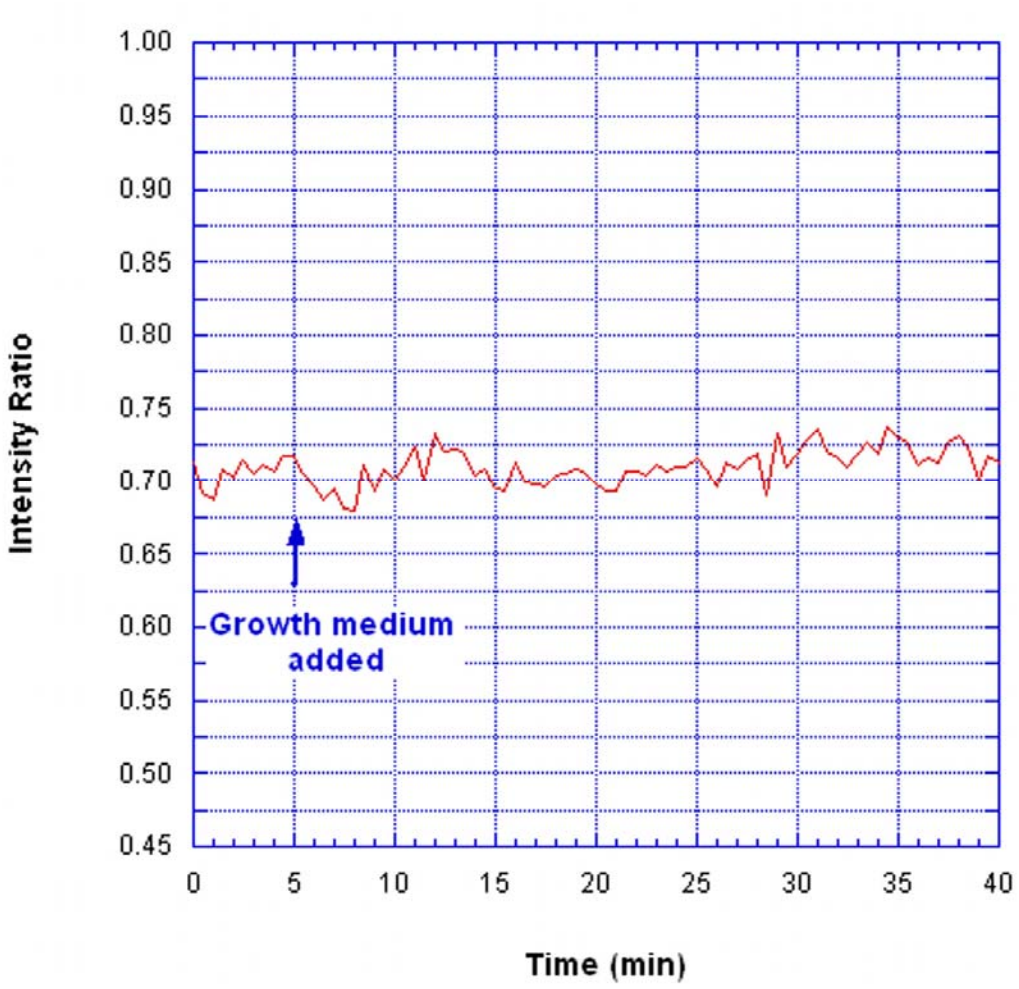

Figure 4.9 Representative graph of cytoplasmic calcium ratios after addition of Gamborg's media. The hairs were imaged every 30 s. No significant change was seen in the ratios.

4.5.2. Response of cytosolic calcium to control medium

Table 4.5 represents the number of experiments in which only Gamborg's medium was perfused over the plants. Images were recorded at 5 s intervals. Averages and standard deviations were calculated and shown in Table 4.5, which results from data from 5 separate root hairs. The cytoplasmic calcium level did not change in response to control medium (Figure 4.10).

Table 4.5 Data obtained from addition of Gamborg's media as a control to RKN addition.

Root Hair Number	Ratio change for 0-1 min measurements	Ratio change for 17-22 min measurements	Intensity ratio change
1	0.4960 ± 0.005	0.513 ± 0.011	0.016
2	0.4571 ± 0.02	0.472648 ± 0.005	0.014
3	0.5326 ± 0.01	0.550018 ± 0.012	0.017
Mean change in intensity ratio			**0.015 ± 0.001**

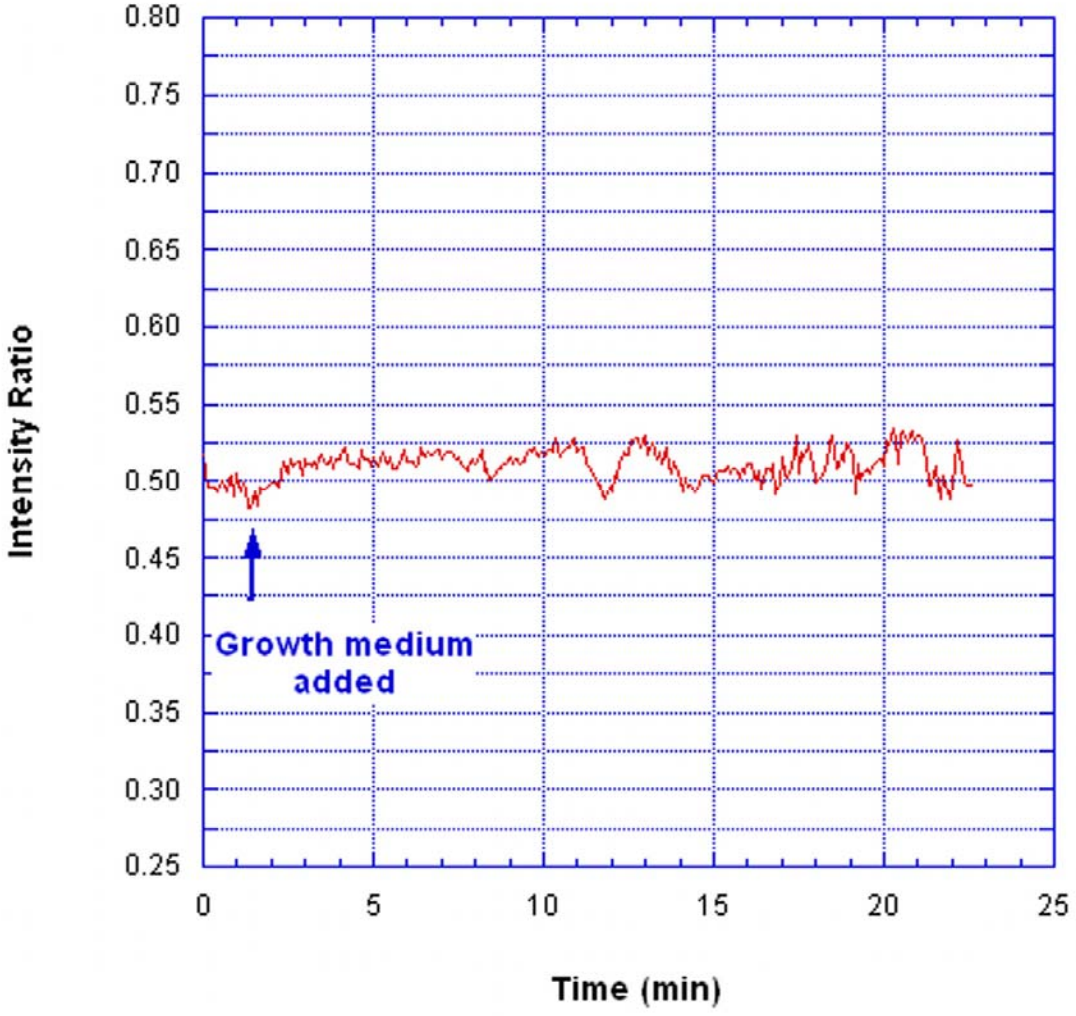

Figure 4.10 Change of intensity ratio in *L. japonicus* root hairs over the nuclear area in response to Gamborg's media.

4.5.3. No Change of cytosolic calcium is seen over the nuclear area 15 - 30 min after media addition.

For 15-30 min the calcium levels did not changed in response to medium perfusion (Figure 4.11).

Table 4.6 Summary of data obtained from addition of media. After addition of medium, imaging was carried out for 1 min. Then the slide was kept in the dark for 15 min before imaging was resumed.

Root Hair Number	Ratio change for 0 -1 min measurements	Ratio change for 16.5 - 21.5 min measurements	Change intensity ratio
1	0.5444 ± 0.006	0.5431 ± 0.010	-0.011
2	0.5784 ± 0.011	0.5935 ± 0.009	0.015
3	0.5105 ± 0.010	0.5058 ± 0.011	-0.004
4	0.5125 ± 0.010	0.5061± 0.008	-0.006
Mean change in intensity ratio			**0.006 ± 0.009**

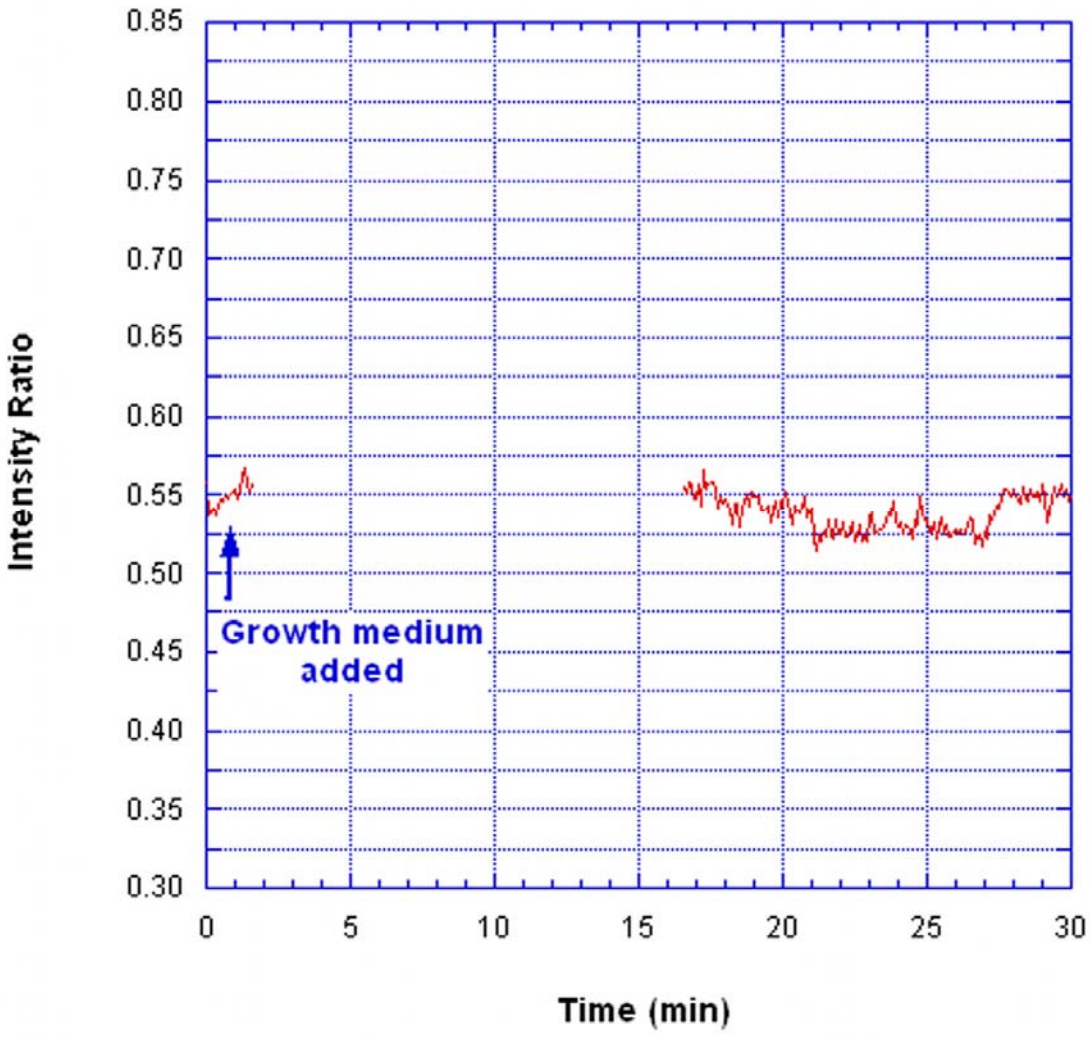

Figure 4.11 Response of cytoplasmic calcium levels over nuclear area to perfusion of medium. No change in calcium level was seen over the imaging period.

4.5.4. Effect of Nod factor treatment on cytoplasmic calcium of *L. japonicus* root hairs

In order to observe whether Indo-1 can successfully represent the cytoplasmic calcium changes, Indo-1 loaded root hairs were imaged for one minute and then treated with 100 nM Nod factor (Table 4.7) with imaging continuing 1 frame every 3 s for 3 min. Imaging was resumed at 9 min to observe the later changes to the initial ratio. This gap in imaging was necessary because of photobleaching problems. The calcium level rapidly increased after 2-5 min and remained constant from 9-19 min after NF addition. Calcium levels declined slightly after 19 min (Figure 4.12)**.** Overall the mean intensity ratio change was 0.084 or 155 nM.

Table 4.7 Change in intensity ratios observed over time after Nod factor treatment of *L. japonicus* root hairs.

Root hair number	Ratio change for 0-1 min measurements	Ratio change For 25-30 min measurements	Increase in intensity ratio
1	0.6234 ± 0.007	0.6973 ± 0.020	0.064
2	0.6324 ± 0.008	0.7303 ± 0.010	0.098
3	0.5814 ± 0.006	0.6720 ± 0.010	0.091
Mean change in intensity ratio			**0.084 ± 0.01**

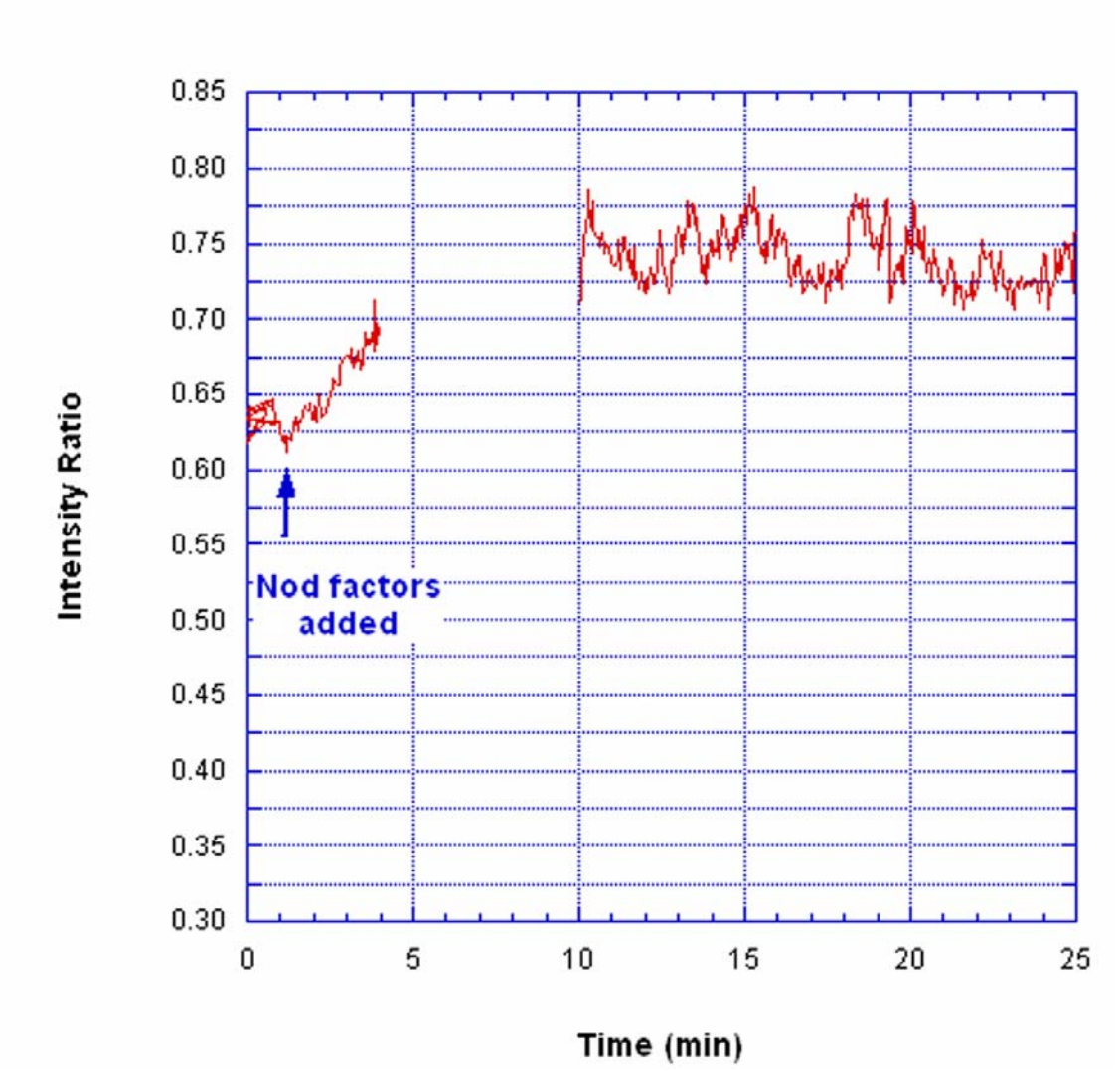

Figure 4.12 Increase in cytoplasmic calcium is evident in response Nod factors.

4.5.5. Cytoplasmic calcium increases in *L. japonicus* root hairs exposed to RKN *M. Incognita*

The cytoplasmic calcium changes after addition of RKN were monitored in Indo–1 loaded wild type *L. japonicus* root hair cells (Table 4.8). Figure 4.13, a representative experiment, shows an increase in intensity after addition of RKN. The images were obtained every 30 s for 30 min. After establishing a baseline ratio for 5 min, RKN was perfused into the chamber and imaging was done continuously. The response was observed after about 4 min of RKN addition (Figure 4.13). Calcium levels continue to increase for the next 15-20 min with a mean average of 0.142 units of intensity ratio. A significant difference in cytoplasmic calcium levels (263 nM) at the tip area of the *L. japonicus* root hairs was observed compared to control Gamborg's media (Figure 4.9) perfusion ($P = 0.001$).

Table 4.8 The data recorded from the addition of RKN *M. incognita* to *L. japonicus* root hairs.

Root hair number	Ratio change for 0-5 min measurements	Ratio change for 25-30 min measurements	Increase in intensity
1	0.9321 ± 0.020	1.1481 ± 0.020	0.105
2	0.5896 ± 0.020	0.7993 ± 0.040	0.109
3	0.8051 ± 0.033	1.0254 ± 0.033	0.220
4	0.7517 ± 0.040	0.9447 ± 0. 030	0.172
5	0.5286 ± 0.006	0.6358 ± 0.011	0.106
Mean change in intensity ratio			**0.142 ± 0.050**

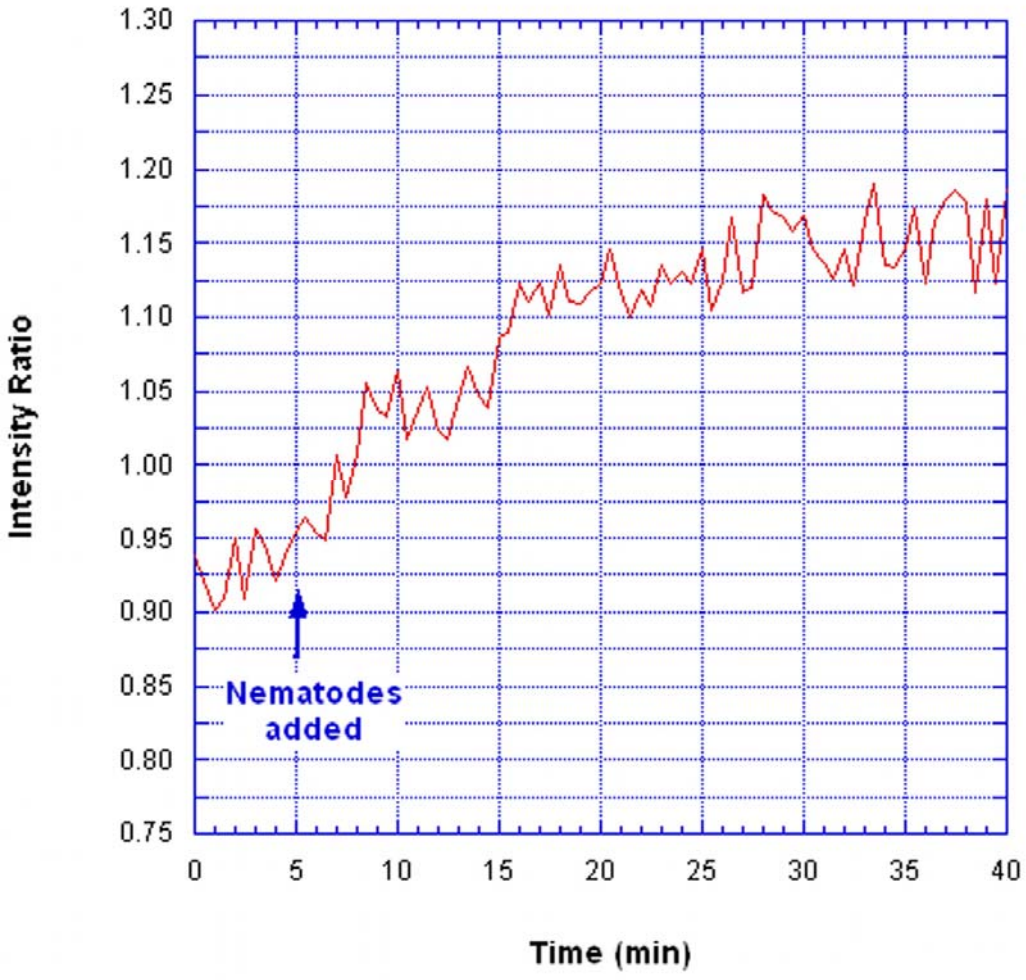

Figure 4.13 Cytoplasmic calcium change in response to the nematode *M. incognita*. Calcium intensity ratios increased 0.22 in the presence of RKN at the root hair tip area 10min after RKN addition. The images were obtained every 30 s for 30 min.

4.5.6. Cytoplasmic calcium increases over the nucleus of *L. japonicus* root hairs after Nod factor addition

Nod factor addition caused calcium spiking over the nucleus of root hairs at different time frames. The spiking response was seen in two root hairs. In one it started as early as 6 min after Nod factor addition in the other case it occurred 17 min after addition (Figure 4.14). The classical spiking pattern (Figure 4.15) in which the spiking occurs at regular one-minute intervals was observed but not in every case. The peak heights showed about 0.02 increase of intensity ratio where base values were less than 0.005 intensity ratio units.

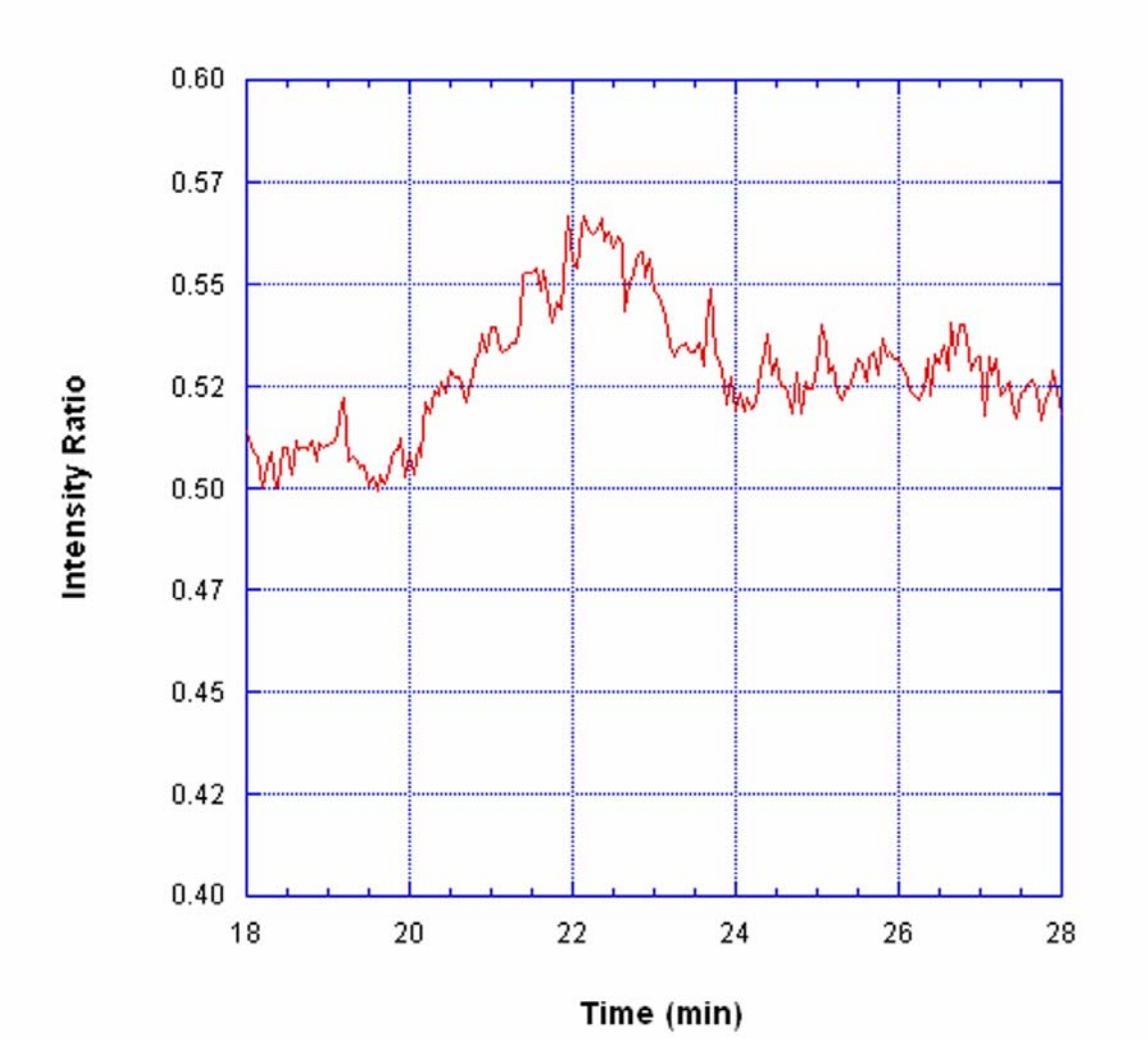

Figure 4.14 Change of intensity ratio in *L. japonicus* root hairs over the nuclear area in response to Nod factors. Nod factor was added after 1 min of imaging.

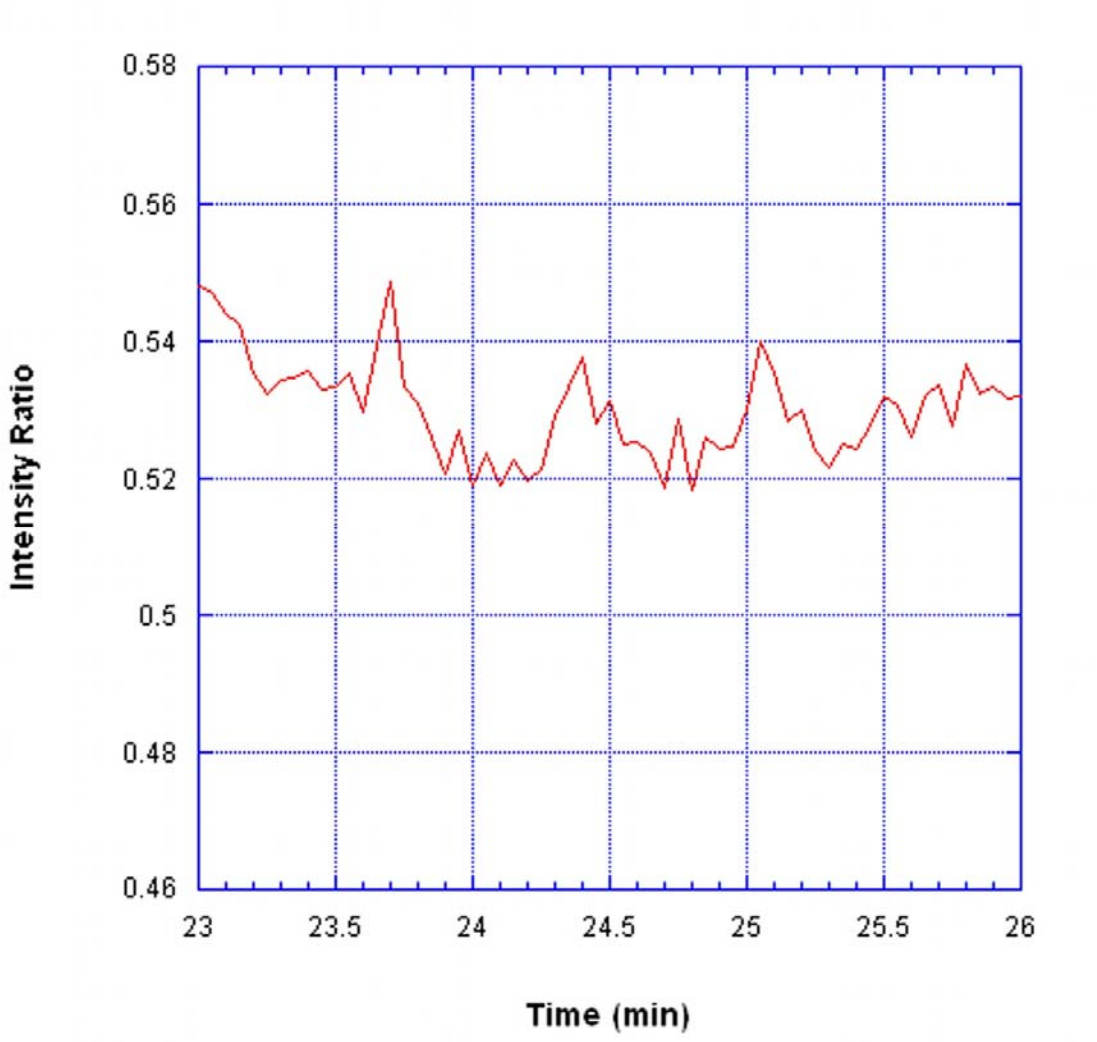

Figure 4.15 Magnified area from 23-26 min from Figure 4.14 demonstrating the classical calcium spiking seen one minute apart over the nuclear area of root hairs.

4.5.7. Cytoplasmic calcium levels of root hairs are altered after exposure to RKNs

A steady state calcium level was measured and then root hairs were perfused with RKN containing medium (Table 4.9). The calcium levels started to increase after about three min and remained high for 21 min. Calcium spiking was not observed within the experimental periods (Figure 4.16). The mean increase of intensity ratio was 0.078 or 144 nM.

Table 4.9 RKN treatments cause a change in intensity ratios indicating that calcium levels were elevated.

Root Hair Number	Ratio change for 0-50 s measurements	Ratio change for 16 -21 min measurements	Increase in intensity ratio
1	0.4000 ± 0.001	0.4800 ± 0.013	0.080
2	0.3802 ± 0.01	0.4409 ± 0.020	0.061
3	0.4817 ± 0.02	0.5705 ± 0.010	0.091
4	0.6093 ± 0.02	0.5355 ± 0.009	0.074
5	0.5515 ± 0.01	0.6397 ± 0.020	0.088
Mean change in intensity ratio			**0.078 ± 0.01**

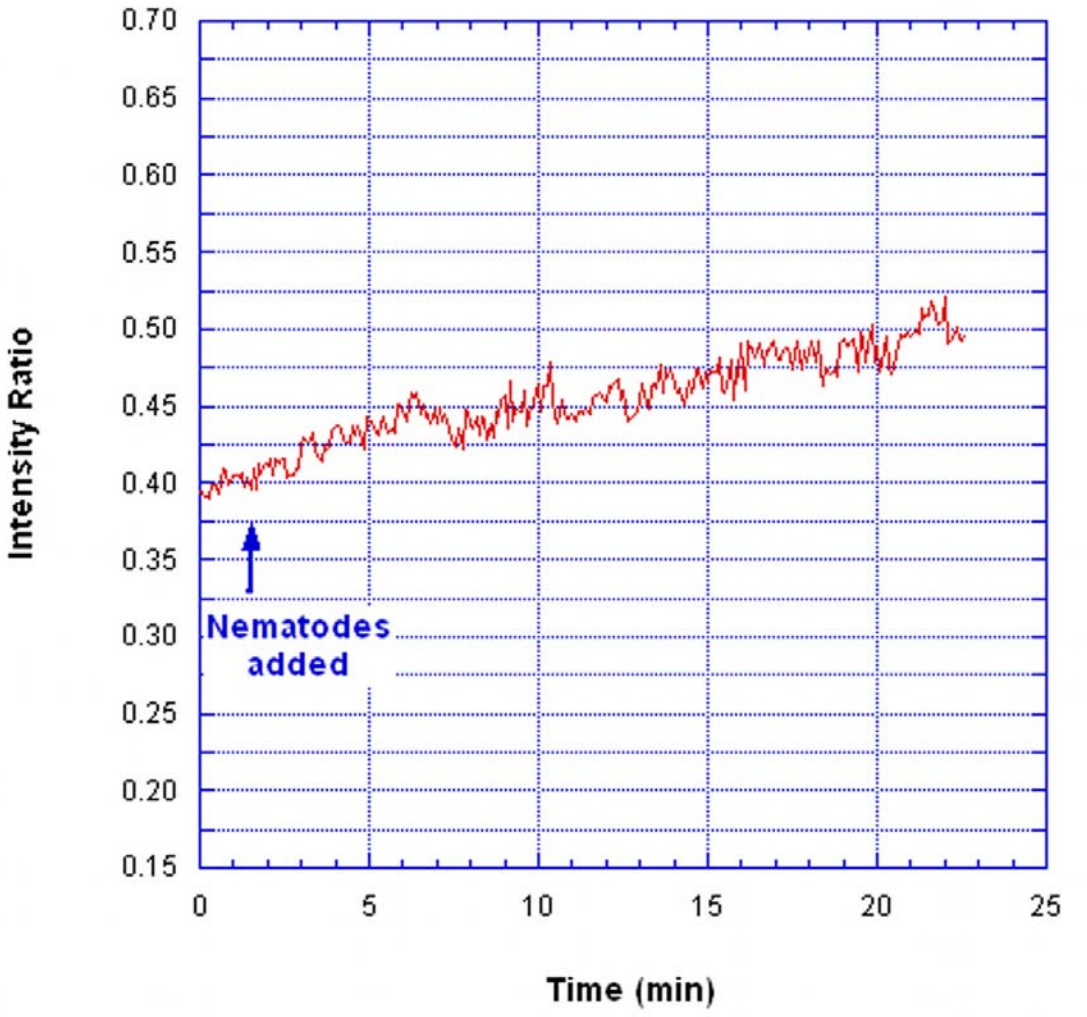

Figure 4.16 Change of intensity ratio over the nuclear area of *L. japonicus* root hairs in response to RKN. The RKNs were added at arrow. Images of Indo-1 loaded growing root hairs were taken at 1 frame every 5 s.

4.5.8. Cytosolic calcium over the nucleus increases after 15 min of RKN treatment

In order to establish the time course of the calcium change in response to RKNs, the imaging period was extended by starting the imaging 15 min after RKN addition. It was not possible to collect images for very long time duration as the Indo-1 fades due to photobleaching. Table 4.10 presents the data obtained from these experiments. The cytoplasmic calcium level over the nucleus remained high from 15-30 min after RKN perfusion (Figure 4.17). This level of calcium was significantly different (P= 0.00002) compared to the control (Figure 4.11).

Table 4.10 Data obtained from addition of RKN over the nuclear area. After addition of RKN, imaging was carried out for 1 min and then 15 min interval was kept before starting imaging again.

Root Hair Number	Ratio change for 0-1 min measurements	Ratio change for 16.5-21.5 min measurements	Increase in intensity ratio
1	0.4370 ± 0.003	0.0492± 0.011	0.060
2	0.3866 ± 0 .003	0.4767 ± 0.011	0.090
3	0.4617 ± 0.004	0.5641 ±0.010	0.102
4	0.4391 ± 0.003	0.5589 ± 0.019	0.119
5	0.4630 ± 0.002	0.5881 ± 0.011	0.125
Mean change in intensity ratio			**0.099 ± 0.02**

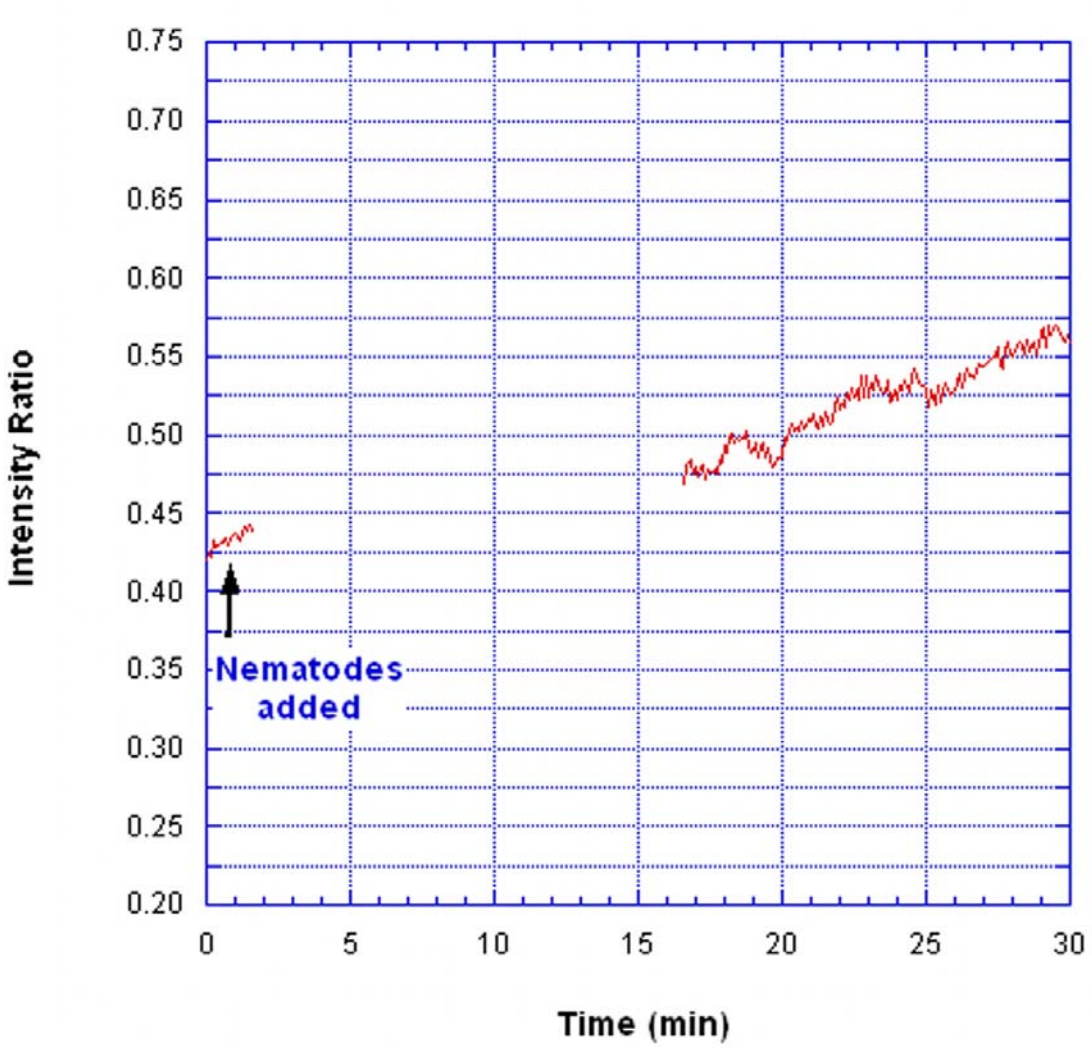

Figure 4.17 Change of intensity ratio over the nuclear area in *L. japonicus* root hairs in response to RKN perfusion. RKN were added to the root hairs and imaged 15 min after addition.

Table 4.11 represents the number of experiments carried out with respect to each treatment. The experiments that had an increase of calcium concentration in the cytoplasm were considered as successful experiment in treatment. For Gamborg's media addition, the experiments that did not show a calcium increase with time were considered as successful experiments. Since each experiment imaged different numbers of root hairs, the two right most columns represent the number of root hairs, which showed a response out of total number of root hairs analyzed in each experiment.

Table 4.11 Total number of experiments performed and number of successful experiments.

Experiment	Total number of experiments carried out	Number of successful experiments	Total number of root hairs in each experiment	Number of root hairs with indicated response
A23187	6	5	14	11
Mas-7	6	1	9	1
Nod factor at the tip	3	3	5	5
Control at the tip 30s interval imaging	9	7	10	8
Control for 5s image acquisition over the nuclear area	7	5	7	5
Control for 5s image acquisition over the nuclear area after 15 min	3	3	7	6
RKN addition 30s image acquisition over the tip area	8	7	14	10
RKN addition for 5s image acquisition over the nuclear area	4	4	6	6
RKN addition for 5s image acquisition over the nuclear area after 15 min	4	4	9	8

5. DISCUSSION

5.1. The common pathway between symbiotic rhizobia, Mycorrhiza and parasitic RKN

Plants and animals have developed different strategies to overcome environmental stresses. An example of one such highly successful method is the symbiosis that occurs between plants and microorganisms, which benefits both the plant and the interacting organism. rhizobia when present in soil with limited nitrogen condition will induce legumes to form nodules hosting rhizobia in the form of bacteroids. Mycorrhiza, another symbiotic organism, form an arbuscule with a highly branched network of hyphae in the roots of most higher plants. In addition, a highly successful parasitic interaction occurs between endoparasitic nematodes and plants. In this case, the plant developmental pathway is altered by signals emanating from the nematode (Weerasinghe et al. 2005).

The existence of a common pathway between symbiotic rhizobia, mycorrihza and parasitic nematodes during their invasion of plants is an interesting phenomenon to explore. Induction of multicellular structures by both symbiotic organisms and parasitic nematodes provides a researcher with a common foundation to explore the early responses leading to formation of these structures. This process starts by communication between the organisms at a distance and ends after establishment of nodules or feeding sites in the plant by the symbiotic or parasitic organism. As reviewed in the introduction, many of the early physiological and morphological changes that occur during the rhizobial nodulation process have been reported. Therefore, it will be important to determine what the nature of early physiological and morphological changes are in the process of nematode invasion and to compare these with what happens during the symbiotic events mentioned above.

In this study I am interested in the early physiological changes that occur when the parasitic RKN, *M. incognita* interacts with the legume host *L. japonicus.* These changes have not yet been studied. One of the first reported changes observed during nodulation is a change in cytoplasmic calcium levels in receptive root hairs of the legume. Therefore, I focused on recording possible early changes of cytoplasmic calcium occurring in response to the RKN, M. *incognita* treated *L. japonicus* root hairs.

5.2. Expected ratio changes were not seen with cameleons

Cameleon expressing *L. japonicus* plants, obtained by hairy root transformation, did not show a change in the emission ratio after addition of calcium ionophore A23187, Nod factor or touch stimuli, which have been reported to raise cytosolic Ca^{2+} in this and other systems (Truong et al. 2001). This could be due to the high expression level of cameleons in the root hairs that were used for our experiments since these required a high time resolution (15 ms time intervals). Root hairs with low expression levels did not show any satisfactory emission intensities under our experimental conditions. It is of significant interest that the emission intensity of the FRET channel (channel 2) was high in both wild type and mutant plants (*symRK, nfr1*) and did not change after treatment with various stimuli. This shows that the cameleons were able to FRET. However, the lack of response of the FRET channel intensity to Ca^{2+} changes could indicate that CaM is already saturated with Ca^{2+} before the stimulus was applied. It is conceivable that expression of CaM under the 35S promoter is the cause of

this CaM overexpression. Future work needs to focus on expressing cameleons under a different promoter which might be able to recover the sensitivity of CaM to cytoplasmic Ca^{2+}.

5.3. Validation of Data

5.3.1. Indo-1 reports calcium with an acceptable accuracy

Ratiometric calcium indicators such as Fura-2 and Indo-1 provide excellent tools to map changes in intracellular calcium levels in space and time. Since Indo-1, which was used in this study, has different emission responses at different calcium levels, the ratio of the intensity measured at the peak of the emission at high calcium concentration and the peak at low calcium levels allows reliable assessment of the direction of the calcium change after a stimulus is applied. The ratiometric approach is more accurate than non-ratiometric methods, which do not allow us to distinguish whether changes in the fluorescence intensity reflect a change in calcium concentration or uneven dye distribution. Intensity ratios were calibrated against an Indo-1 solution buffered in defined calcium concentrations (Molecular Probes Calcium Calibration Standards with 1 mM Mg^{2+} to reflect magnesium levels inside the cytoplasm). When compared with the *in vitro* calibration, our ratio measurements indicated higher calcium levels than expected for physiological conditions. The most logical explanation for this is that the chemical environment of the cytosol might shift the emission spectrum of Indo-1 and the only way to account for this shift is to equilibrate the cytoplasm with known calcium standards and perform an *in vivo* calibration. Since we had difficulties

getting the calcium ionophore A23187 to work reliably in our system (4.4.2) an *in vivo* calibration could not be performed, i.e. the internal free calcium concentration did not equilibrate to the same values as the external buffer media (Takahashi et al. 1999). For the reasons outlined above I present the data as ratio changes over time rather than calcium concentration changes. The magnitude of the change in cytosolic calcium can be more accurately deducted from the *in vitro* calibration than the absolute values. Figure 4.6 shows that the *in vitro* calibrations are fairly linear over the physiological calcium concentration range (0-0.6 μM). An increase in intensity ratio from 0.4 to 0.6 corresponds to a change in free calcium concentration of about 370 nM (Indicated by arrows in Figure 4.6). The stimulus induced calcium changes that we deduced using the *in vitro* calibration fell within the expected range.

5.3.2. Calcium Ionophore A23187 increased the cytoplasmic calcium level in indo-1 loaded *L. japonicus* root hairs

Ionophores increase the permeability of cell membranes either by forming a channel, through which ions can move, or they act as an ion carrier (Arslan et al. 1985). We use calcium ionophore A23187, an artificial ion carrier that acts as an ion exchange molecule to deliver calcium ions into the root hair cells. A23187 consists of a hydrophobic region and a hydrophilic region. The hydrophobic region makes it lipid soluble and allows it to enter membranes. The hydrophilic region binds ions and redistributes the charge of the molecule so that it is sheltered from hydrophobic regions of the membrane allowing it permeate into the membrane. A23187 transports one calcium ion into the cell in exchange of two H^+ ions

(Balasubramanian, 1992). Root hairs treated with A23187 at pH =7.2 with external 20 mM Ca^{2+} had an increase in intracellular calcium level 15 min after application of A23187, the internal Ca^{2+} level was elevated with a mean ratio change of 0.130 ± 0.04 (Table 4.1) This value corresponds to a 240 nM increase of the calcium level as calculated from an *in vitro* calibration and a 0.1 increase of intensity ratio corresponds to 185 nM (Figure 4.7). I did not observe a sudden elevation of calcium levels as one might expect indicating that the ionophore penetration was incomplete (Legue et al. 1999).

5.3.3. Mastoparan agonist Mas-7 did not elevate the cytosolic calcium level in indo-1 loaded root hairs

Mas-7 is an active cationic synthetic analog of mastoparan, a peptide found in wasp venom. It can be used to elevate intracellular calcium levels (Tucker and Boss, 1996). Mas-7 permeabilizes the plasma membrane allowing ions to move through it to cytoplasm hence can increase the cytoplasmic calcium level immediately. Mas-7 is also an artificial activator of G protein, which is involved in the G protein signaling pathway of plants and animals, by imitating the intracellular domain of membrane spanning receptors. G proteins are found in the plasma membrane facing the cytoplasm and transduce signals from the cell surface to the effector enzymes downstream of G proteins (Hooley, 1998).

Mastoparan and Mas-7 elevate inositol-1,4,5 triphosphate (IP_3), a secondary messenger which acts to release calcium from intracellular stores, thereby raising cytosolic Ca^{2+} in cells. Mas-7 microinjected into *Setcreasea purpurea* cell that contained calcium green dextran, a

nonratiometric Ca^{2+} indicator, enhanced the fluorescence intensity within 30 s and it continued to oscillate for about 3 min (Tucker and Boss, 1996). Mastoparan and Mas-7 were also able to mimic the Nod factor response by inducing early nodulin (ENOD) genes. In *M. truncatula ENOD12,* gene expression in epidermal cells were induced by Mas-7 (Pingret et al. 1998). This expression was inhibited by the G protein antagonist bacterial pertussis toxin. 1μM Mas-7 applied to *Vicia sativa* root hair caused deformations similar to those observed on Nod factor (from *Rhizobium leguminosarum bv*. *Viciae)* treated root hairs (Hartog, 2001). I was unable to detect an elevation of cytoplasmic calcium levels when the root hairs were treated with 7.5 μM active Mas-7. A student t-test with a significance level of 0.05 indicated no significant difference observed in Mas-7 treated root hairs compared to the control roots that were perfused with Gamborg's media (P = 0.47495). The reason for this could be that Mas-7 peptide that was used in this experiment might not have been in good condition and not active, not able to enter the cell membrane of root hairs or failing to activate the G proteins and trigger IP_3 changes and subsequent calcium release from intracellular stores as observed in previously described studies (den Hartog, 2001). den Hartog (2001) reported that external application of Mas-7 for 5 min induced the lipid signaling pathway by inducing phosphatidic acid (PA), which could be detected as early as 2 min and reached a maximum after 10-12 min. In our study Mas-7 was also applied externally within a similar time frame but we did not observe the expected change in cytosolic calcium levels.

5.3.4. Addition of Nod factor causes cytoplasmic calcium increase in the tip area of *L. japonicus* root hairs

Many studies have reported a tip based calcium gradient in tip growing cells, which must be present for growth to occur (Schiefelbein et al. 1992; Pierson et al. 1994; Hermann and Felle, 1995; Brownlee et al. 1999). Since this gradient was only observed in growing cells, it must be intricately associated with tip growth (Pierson *et al* 1994; Allen and Bennett, 1996). Felle et al. (1998) observed a transient calcium influx in the tip of growing root hairs of *M. sativa* in response to Nod factor treatment from *R. meliloti* using electrophysiological methods. It has been implied that this calcium influx might trigger the downstream events of Nod factor signaling (de Ruijter et al. 1999). Felle et al. (1999a) observed a tip based calcium gradient in growing *M. sativa* root hairs where an increase of calcium was observed behind the tip and a decrease at 5-10 μM within the tip. Felle et al. 1999b investigated the requirement of Ca^{2+} for Nod factor signaling and showed that an increase of cytosolic calcium is absolutely necessary for Nod factor signaling. In addition, Cardenas et al. (1999) also illustrated a cytosolic calcium level increase within 5-10 min of Nod factor application and after 10-15 min periodic calcium oscillations in black bean (*Phaseolus vulgaris)*. Gehring et al. (1997) showed an increase in cytosolic calcium in response to Nod factors. A rapid increase of cytosolic calcium within a few seconds was recorded at the cytoplasm of the root hair tip of *Vigna unguiculata* using microscopy and Fura 2 ratio imaging. The experiment with *Arabidopsis*, a non legume nonhost plant failed to show the cytosolic elevation of calcium. de Ruijter et al. (1998) used Indo-1 loaded *Vicia sativa* L. (vetch) root hairs to demonstrate that a tip based calcium gradient existed and that elevation of Ca^{2+} occurred at the tip after addition of Nod factors. The area of calcium influx is thought to influence the location of

actin and microtubules leading to a new growth area and root tip deformations and curling. The calcium increase also leads to other developmental changes. These results collectively indicate an involvement of an increase of cytoplasmic calcium in Nod factor signaling.

In the present study, Nod factors (10^{-7} M) were added to the *L. japonicus* root hairs. (Figure 4.7).

Images of the root hairs were obtained at a rate of 1 frame every 3 s. The results obtained from our study agree with those discussed above. The timing of the increase of tip calcium levels was the same as that observed in Cardenas et al. (1999) occurring after minutes followed by the calcium spiking about 15 min after of Nod factor application. At the tip of the root hairs, a significant difference of change of free calcium levels (263 nM) was observed compared to controls (P=0.001). This clearly indicated that the data obtained using the indo-1 indicators are in agreement with earlier observations and difference compared to published work may be due to species response variations.

5.4. Nematodes cause an increase in cytoplasmic calcium at the tip and over the nucleus of *L. japonicus* root hairs

5.4.1. Cytoplasmic free calcium increases at the root hair tip region after RKN exposure as much as it does after Nod factor exposure

The cytoskeleton plays an important role in root hair tip growth (Bibikova et al. 1999). Weerasinghe et al. 2003 showed that Nod factor treated root hairs of *M. sativa* demonstrated a change in distributional pattern of microtubules (MT). Endoplasmic microtubules start to disintegrate first and then cortical microtubules start to disintegrate at the base of the root

hairs within 3-10 min after perfusion of Nod factor. After 20 min, bands of MTs appear behind the tip and within 30 min almost all the MTs depolymerized. After about one hour the MT cytoskeleton reformed showing the normal distribution pattern. Weerasinghe et al. 2005 reported that the RKN *M. incognita* induced similar actin and microtubule cytoskeletal changes as those induced by Nod factors in *L. japonicus* root hairs. In addition RKN induce the branched and wavy root hairs also seen as a response to Nod factors. These similar changes point to an existence of a common pathway for symbiotic nodule and parasitic root knot gall formation. In this study elevation of cytoplasmic calcium in response to Nod factor was observed in *L. japonicus* root hairs similar to those that have been observed and reported as described in 5.3.4. I detected increases of cytoplasmic calcium in *L. japonicus* root hair tips treated with the RKN *M. incognita* after 2-3 min. A sustained increase of calcium was observed for 20-25 min. This rise in calcium levels is similar to that observed after Nod factor treatment except it is more sustained. The time course and pattern of calcium increase reported in Cardenas et al. in 1999 with respect to Nod factors is very similar to what I report here for RKN. The results indicate that there is a significant difference in cytoplasmic calcium concentration in RKN treated *L. japonicus* root hairs over controls ($P = 0.0001$). The mean calcium concentration increase at the tip area is about 263 nM (Table 4.7). These data shows that RKN as well as Nod factors are able to change the cytoplasmic calcium concentration. The changes can be detected as early as 2 min after application of RKN to the root hairs. At the tip, the calcium level is higher in Nod factor treated than RKN treated root hairs. Further information could be obtained by using the calcium specific ion selective vibrating probe to look at specific calcium influx at the tip of root hairs after RKN addition. The fact that RKN can induce a Ca^{2+} concentration change in roughly the same time frame

and at similar levels to that seen with Nod factors indicates that the receptors sensing RKN likely are similar to the recently reported Nod factor receptors mentioned above. It will be very important to test the Nod factor receptor mutants to see what their responses to RKN would be and compare them to the results obtained with Nod factor challenge.

5.4.2. RKN cause an increase in cytoplasmic calcium over the nucleus of *Lotus japonicus* root hairs

In order to find out if the cytoplasmic calcium change associated with the nuclear area seen after Nod factor exposure also occurs after RKN addition, the nuclear area of the nematode treated root hairs were imaged using confocal laser scanning microscopy. Images were taken at 5 s intervals, as this is a suitable time scale for detecting fairly rapid calcium responses such as the 1 min periodic spiking mentioned in section 4.5.6. Because Indo-1 bleaches during fast image acquisition, imaging over a 30 min period had to be carried out in two steps.

First, imaging was carried out over the nucleus for 20 min after RKN addition. Secondly, initial readings were made, RKN added, and imaging was started at 15 min after the addition of RKN (See figure 4.17). This allowed the imaging at later times without photobleaching.

The cytosolic calcium level rose starting about 3-5 min after RKN perfusion and stayed elevated throughout the experimental period of 25 min. The student t-test verifies that there is a significant difference ($P = 0.00002$) between control media addition (Table 4.13 and Figure 4.13) and RKN perfusion (Table 4.11 and figure 4.12).

The increase in mean calcium concentration 22 min after nematode addition was about

0.078 intensity ratio units which is equivalent to 142 nM of free calcium. The jump in intensity ratio during the 15 min period the experiment was stopped is in close agreement with the change I observed in parallel experiment in which I monitored the response continuously for 15-20 min (see section 4). Interestingly, after 15 min of nematode treatment I observed a rise in the free calcium concentration over the nuclear area. After about 25-30 min of RKN addition, the calcium level remained at a higher concentration.

In case of Nod factor application regular calcium spiking was observed after about 10 min in the studies with *L. japonicus* (Harris et al. 2003). We did not detect calcium spiking over the nuclear area of RKN treated root hairs over the total measured 30 min period, but did detect spiking after Nod factor addition in some cases.

Overall results from my investigations indicate a sustained increase of calcium at the root hair tip and over the nuclear area in *L. japonicus* root hairs treated with RKN *M. incognita*. This is the first time to our knowledge, that an increase of cytoplasmic calcium has been detected as a response to RKN treatment. This study provides a basis for further investigation to elucidate the common paths and branching points of symbiotic and parasitic signaling pathways in nodule and root knot formation. Data from the RKN treatment indicate increases of cytoplasmic calcium levels, which are very similar temporally and spatially to the calcium changes observed during nodulation. Therefore I postulate that RKN parasitism also employs changes in calcium ion fluxes early in the signal transduction pathway leading to successful giant cell formation. It is important now to see if proton levels also change with a time course similar to that seen with Nod factors, since protons have also been suggested to act as secondary messengers (Scott and Allen. 1999). Both ratio dyes, GFP pH indicators and

proton biocurrent probe methods should be employed to see if the RKNs change the cytoplasmic pH levels in root hairs.

This study suggests that the early changes in successful nematode parasitism use calcium, which acts as a secondary messenger in response to many environmental stimuli including rhizobia (Sanders et al. 1999). This also is further evidence that symbiotic rhizobia, mycorrhiza and parasitic nematodes share the early part of their signaling pathway since all have changes in cytosolic calcium and some in pH. More work is needed to further our understanding of this process and elucidate its similarity and difference to the nodulation process. The Nod factor mutants, *nfr1, nfr5* and *symRK* need to be tested to see if their proton and calcium concentration responses to RKN are similar to known Nod factor responses. The three nod factor receptor mutants might respond in different ways shedding light on their respective roles in the signaling pathways of RKN response in plants. Since Nematodes also attack non-leguminous plants, it is clear that we need to look at least at tomato and *Arabidopsis* to determine if they have a proton and calcium response to nematodes (Weerasinghe et al. 2005).

5. REFERENCES

Abad P, Favery B, Rosso MN, Castagnone-Sereno P (2003) Root-knot nematode parasitism and host response: molecular basis of a sophisticated interaction. Mol Plant Pathol 4: 217- 224

Allen GJ, Chu SP, Harrington CL, Schumacher K, Hoffmann T, Tang YT, Grill E, Schroeder JI (2001) A defined range of guard cell calcium oscillation parameter encodes stomatal movements. Nature 411: 1053-1057

Allen GJ, Chu SP, Harrington CL, Schumacher K, Zhimasaki CT, Vafeados D, Kemper A, Hawke SD, Tallman G, Tsien RY, Harper JF, Chory J, Schroeder JI (2000) Alteration of stimulus-specific guard cell specific calcium oscillations parameters encodes stomatal movements. Science 289: 2338-2342

Allen NS, Bennett MN (1996) Electro-optical imaging of F-actin and endoplasmic reticulum in living and fixed plant cells. Scan Microsc Suppl 10: 177- 187

Allen NS, Bennett MN, Cox DN, Shipley A, Ehrhardt DW, Long SR (1994) Effects of Nod factors on alfalfa root hair Ca^{++} and H^{+} currents on cytoskeleton behavior. In MJ Daniels, JA Downie, AE Osbourn, eds, Advances in molecular genetics of plant-microbe interactions, Vol 3. Kluwer Academic Press, Dordecht, pp 07-114

Ardourel M, Demont N, Debellé FD, Maillet F, de Billy F, Promé JC, Dénarié J, Truchet G (1994) *Rhizobium meliloti* lipooligosaccharide nodulation factors: different structural requirements for bacterial entry into target root hair-cells and induction of plant symbiotic developmental responses. Plant Cell 6: 1357-1374

Arslan P, Virgileo F, Beltrame M, Tsien RY, Pozant T (1985) Cytosolic Ca^{2+} homeostasis in Ehrlich and Yoshida carcinomas. A new, membrane permeant chalator of heavy metals reveals that these ascites tumor cell lines have normal cytosolic free Ca^{2+}. J Bio Chem 260: 2719-2727

Balasubramanian SV, Sikdar SK, Easwaran KRK, (1992) Bilayers containing calcium ionophore A23187 form channels. Biocheml Biophys Res Commu 189: 1038-42

Berridge MJ, Bootman MD, and Lipp, P (1998**)** Calcium –a life and death signal. Nature 395: 645-648

Bibikova TN, Blancaflor EB, Gilroy S (1999) Microtubule regulate tip growth and orientation in root hairs of *Arabidopsis thaliana.* Plant J 17: 657-665

Bird AF (1973) Observations on chromosomes and nucleoli in syncytia induced by *Meloidogyne javanica*. Physiol Plant Pathol 3: 387-391

Bird D McK, Kaloshian I (2003) Are roots special? Nematodes have their say. Physiol Mol Plant Pathol 62: 115-123.

Brewin NJ (1991) Development of the legume root nodule. Annu Rev Cell Biol 7: 191-226

Brownlee C, Goddard H, Hetherington Am, Peake LA (1999) Specificity and integration of responses: Ca^{2+} as a signal in polarity and osmotic regulation. J Exp Biol 50:1001-1011

Brundrett M (2002) Coevolution of roots and mycorrhizas of land palnts. New Phytol 154: 275-304

Bush DS (1993) Regulation of cytosolic calcium in plants. Plant Physiol 103: 7-13

Cárdenas L, Vidali L, Domínguez J, Pérez H, Sánchez F, Hepler P, Quinto C (1998) Rearrangement of actin microfilament in plant root hairs responding to *Rhizobium etli* Nodulation signals. Plant Physiol 116: 871-877

Crespi M, Gálvez S (2000) Molecular mechanisms in root nodule development. J Plant Growth Regul 19: 155-166

Cllimore JV, Ranjeva R, Bono JJ (2001) Perception of lipo-chitooligosaccharidic Nod factors in legumes. Trends Plant Sci 6: 24-30

Dénarié J, Debellé F, Rosenberg C (1992) Signaling and host range variation in nodulation. Ann Rev Microbiol 46: 497-531

den Hartog M, Musgrave A, Munnik MT (2001) Nod factor induced Phosphatidic acid and diacylglycerol pyrophosphate formation: a role for phopholypase C and D in root hair deformation. Plant J 25: 55-65

de Ruijter NCA, Bisseling T, Emons AMC (1999) Rhizobium nod factors induce and increase in sub-apical fine bundles of actin filaments in *Vicia sativa* Root Hairs within minutes. MPMI 12: 829-832

Downie JA, Walker S (1999) Plant responses to Nodulation factors. Curr Opin Plant Biol 2: 483-489

Ehrhardt DW, Wais R, Long SR (1996) Calcium spiking in plant root hairs responding to *Rhizobium* nodulation signals. Cell 85: 673-681

Ehrhardt DW, Atkinson EM, Long SR (1992) Depolarization of Alfalfa root hair membrane potential by *Rhizobium meliloti* Nod factors. Science 256: 998-1000

Esseling JJ, Emons AMC (2003) Dissection of Nod Factor signalling in legumes: Cell biology, mutants and pharmacological approaches. J Microsc 214: 104-113

Favery B, Complainville A, Vinardell JM, Lecomte P, Vaubert D, Mergaert P, Kondorosi A, Kondorosi E, Crespi M, Abad P (2002) The endosymbiosis-induced genes ENOD40 and CCS52a are involved in endoparasitic-nematode interactions in *Medicago truncatula*. Mol Plant Microbe Interact 15: 1008-1013

Felle HH (1988) Auxin causes oscillations of cytosolic free calcium and pH in *Zea mays* coleoptiles. Planta 174: 495-499

Felle HH, Kondorosi E, Kondorosi A, Schultze M (1995) Nod signal-induced plasma membrane potential changes in alfalfa root hairs are differentially sensitive to structural modifications of the lipochitooligosaccharides. Plant J 7: 939-947

Felle HH, Kondorosi E, Kondorosi A, Schultze M (1998) The role of ion fluxes in Nod factor signaling in *Medicago sativa.* Plant J 13: 455-463

Felle HH, Kondorosi E, Kondorosi A, Schultze M (1996) Rapid alkalinization in alfalfa root hairs in response to rhizobial lipochitooligosaccharide signals. Plant J 10: 295-301

Fisher RF, Long SR (1992) Rhizobium- plant signal exchange. Nature 357: 655-659

Gehring CA, Irving HR, Kabbara AA, Parish RW, Boukli NM, Broughton WJ (1997) Rapid plateau-like increases in intracellular free calcium are associated with Nod-factor-induced root-hair deformation. Mol Plant Microbe Interact 10: 791-802

Goverse A, Englar JD, Verhees J, Krol S van der, Helder J, Gheysen G (2000) Cell cycle activation by parasditic nematodes. Plant Mol Biol 43: 747-761

Grundler FMW, Sobczak M, Golinowski W (1998) Formation of wall openings in root cells of *Arabidopsis thaliana* following infection by the plant-parasitic *Heterodera schachtii*. Eur J Plant Pathol 104: 545-551

Harris JM, Wais R, Long SR (2003) Rhizobium-induced calcium spiking in *Lotus japonicus.* Am Phytopathol Soc 16: 335-341

Harrison MJ (1999) Molecular and cellular aspects of the arbuscular mycorrhizal symbiosis. Annu Rev Plant Physiol Plant Mol Biol 50: 361-389

Hermann A, Felle HH (1995) Tip growth in root hair cells of *Sinapis alaba* L.: significance of internal and external Ca^{2+} and pH. New Phytol 129:523-533

Hirsch AM, Lum MR, Downie JA (2001) What makes the rhizobia-Legume symbiosis so special? Plant Physiol 127: 1484- 1492

Hooley R (1998) Plant hormone perception and action: a role for G-protein signal transduction? Phil Trans R Soc Lond B 353: 1425-1430

Horvath B, Heidstra R, Lados M, Moerman M, Spaink HP, Prome JC, Van Kammen A, Bisseling T (1993) Lipo-oligosaccharides of *Rhizobium* induce infection-related early nodulin gene expression in pea root hairs. Plant J 4: 727-733

Hussey RS, Mims CW (1991) Ultrastructure of feeding tubes in giant-cells induced in plants by the root-knot nematode *Meloidogyne incognita*. Protoplasma 162: 99- 107

Jones MGK (1981) Host cell responses to endoparasitic nematode attack: Structure and function of giant cell and syncytia. Ann Appl Biol 97: 353-372

Jones MGK, Payne HL (1978) Early stages of Nematode-induced giant cell formation in roots of *Impatiens balsamina*. J Nematol 10: 70-84

Journet EP, Pichon M, Dedieu A, De Billy F, Truchet G, Barker DG (1994) *Rhizobium meliloti* Nod factors elicit cell-specific transcription of ENOD12 gene in transgenic alfalfa. Plant J 6: 241-249

Jung C, Wyss U (1999) New approach to control plant parasitic nematodes. Appl Microbiol Biotechnol 51: 439-446

Kistner C, Parniske M (2002) Evolution of signal transduction in intracellular symbiosis. Trends Plant Sci 7: 511-518

Knight H, Knight MR (2000) Imaging spatial and cellular characteristics of low temperature calcium signature after cold acclimation in *Arabidopsis.* J Exp Bot 51: 1679-1686

Koenning SR, Overstreet C, Noling JW, Donald PA, Beker JO, Fortman BA (1999) Survey of crop losses in response to phytoparasitic nematodes in the United States for 1994. J Nematol 31: 1203-1212

Koltai H, Dhandaydham M, Opperman C, Thomas J, Bird D McK (2001) Overlapping plant signal transduction pathways induced by a parasitic nematode and a rhizobial endosymbiont. Mol Plant Microbe Interact 14: 1168-1177

Kurkdjian AC (1995) Role of differentiation root epidermal cells in Nod factor (from *Rhizobium meliloti*)-induced root hair depolarization of *Medicago sativa*. Plant Physiol 107: 783-790

Legue V, Blancaflor E, Wymer C, Perbal G, Fantin D, Gilroy S (1997) Cytoplasmic free Ca^{2+} in Arabidopsis roots changes in response to touch but not to gravity. Plant Physiol 114: 789-800

Lerouge P, Roche P, Faucher C, Maillet F, Truchet G, Prome JC, Denarie J. (1990) Symbiotic host-specificity of *Rhizobium meliloti* is determined by a sulphated and acylated glucosamine oligosaccharide signal. Nature 344:781-784

Lhuissier FGP, De Ruijter NCA, Sieberer BJ, Esseling JJ, Emons AMC (2001) Time course of cell biological events evoked in legume root hairs by *Rhizobium* Nod factors: state of the art. Ann Bot 87: 289-302

Malhó R (1999) Coding information in plant cells: the multiple roles of Ca^{2+} as a second messenger. Plant Biol 1: 487-494

Miller DD, de Ruijter NCA, Bisseling T and Emons MC (1999) The role of actin in root hair morphogenesis: Studies with lipochito-oligosaccharide as growth stimulator and cytochalasin as an actin perturbing drug. Plant J 17: 141-154

Miyawaki A, Llopis J, Heim R, McCaffery JM, Adams JA, Ikura M, Tsien RY (1997) Flourescent indicators for Ca^{2+} based on green fluorescent proteins and calmodulin. Nature 388: 822-887

Munns DN (1970) Nodulation of *Medicago sativa* in culture v. calcium and pH requirements during infection. Plant Soil 32: 90-102

Orion D, Frank A (1990) An electron microscopy study of cell wall lysis by *Meloidogyne javanica* gelatinous matrix. Rev Nematol 13: 105-107

Pierson ES, Denorah DM, Callaham DA, Shipley AM, Rivers BA, Crest M, Hepler K (1994) Pollen tube growth is coupled to the extracellular calcium ion flux and the intracellular calcium gradient: Effect of BAPTA-Type buffers and hypertonic media. Plant Cell 6: 1815-1828

Pingret JL, Journet EP, Barker DG (1998) Rhizobium Nod factor signaling: evidence for a G-protein mediated transduction mechanism. Plant cell 10: 659-671

Radutoiu S, Madsen LH, Madsen EB, Felle HH, Umehara Y, Grønlund M, Sato S, Nakamura Y, Tabata S, Sandal N, Stougaard J (2003) Plant recognition of symbiotic bacteria requires two LysM receptor like kineses. Nature 425: 585-592

Roche P, Lerouge P, Ponthus C, Prome JC (1991) Structural determination of bacterial nodulation factors involved in the *Rhizobium meliloti*-Alfalfa symbiosis. J Biol Chem 266: 10933-10940

Sanders D, Brownlee C, Harper JF (1999) Communicating with calcium. Plant cell 11: 691-706

Sasser JN, and Freckmsn DW (1987) A world perspective of on nematology: The role of society. In JA Veech, DW Dickson, eds, Vistas on Nematololgy. Soc Nematol Inc., Hyattsville, pp 7-14.

Sathyanarayanan PV, Poovaiah BW (2004) Decoding Ca^{2+} signal in plants. Crit Rev Plant Sci 23: 1-11

Schauser L, Handberg K, Sandal N, Stiller J, Thykjaer T, Pjuelo E, Nielsen A and Stougaard J (1998) Symbiotic mutants deficient in nodule establishment identified after T-DNA transformation of *Lotus japonicus*. Mol Gen Genet 259: 414-423

Schiefelbein JW, Shipley A, Rowse P (1992) Calcium influx at the tip of growing root hair cells of *Arabidopsis thaliana.* Planta 187: 455-459

Scott AC, Allen NS (1999) Changes in cytosolic pH within *Arabidopsis* root columella cells play a key role in the early signaling pathway for root gravotropism. Plant Physiol 121: 1291-1298

Shaw SL, Long SR (2003) Nod Factor elicits two separable calcium responses in *Medicago truncatula* root hair cells. Plant Physiol 131: 976-984

Spaink HP, Sheeley DM, van Brussel AAN, Glushka J, York WS, Tak T, Geiger O, Kennedy EP, Reinhold VN, Lugtenberg BJJ (1991) A novel highly unsaturated fatty acid moiety of lipo-oligosaccharide signals determines host specificity of *Rhizobium*. Nature 354: 125-130

Staehelin C, Granado J, Muller J, Wiemken A, Mellor RB, Felix G, Regenass M, Broughton WJ, Boller T (1994) Perception of *Rhizobium* nodulation factors by tomato cells and inactivation by root chitinases. Proc Natl Acad Sci USA 91: 2196-2200

Stiller J, Martirani L, Tuppale S, Chian RJ, Chiurazzi M, Gresshoff PM (1997) High frequency transformation and regeneration of transgenic plants and the model legume *Lotus japonicus.* J Exp Biol 48: 1357-1365

Stracke S, Kistner C, Yoshida S, Mulder L Sato S, Kaneko S, Sandal N, Stougaard J, Szczyglowski K, Parneske M (2002) A plant receptor-like kinase is required for both bacterial and fungal symbiosis. Nature 417: 959-962

Takahashi A, Camacho P, Lechleiter JD, Herman B (1999) Measurement of intracellular calcium. Physiol Rev 79: 1089-1125

Timmers ACJ, Auriac M-C, Truchet G (1999) Refined analysis of early symbiotic steps of the *Rhizbium-Medicago* interaction in relationship with microtubular cytoskeleton rearrangements. Development 126: 3617-3628

Trewavas A (2000) Signal perception and transduction. In BB Buchanan, W Gruissem, RL Jones, eds, Biochemistry and molecular biology of plants, Ed 1. Am Soc Plant Physiol, Rockville, pp 962-973

Trudgill DL, Block VC (2001) Apomictic, polyphagous root-knot nematodes: Exceptionally successful and damaging biotrophic root pathogens. Annu Rev Phytopathol 39: 53-77

Truong K, Sawano A, Mizuno H, Hama H, Tong KI, Mal TK, Miyawaki A, Ikura M (2001) FRET-based in vivo Ca^{2+} imaging by a new calmodulin – GFP fusion molecule. Nat Str Biol 1-5

Tucker EB, Boss WF (1996) Mastoparan- induced intracellular Ca^{2+} fluxes may regulate cell to cell communication in plants. Plant Physiol 111: 459-467

Tzortzakakis EA, Trudgill DL (1996) A thermal time based method for determining the fecundity of *MELOIDOGYNE JAVANICA* in relation to modelling its population dynamics. Nematology 42: 347- 353

Wais RJ, Galera C, Oldroyd G, Catoira R, Penmetsa VR, Cook D, Gough C, Dénarié J, Long S (2000) Genetic analysis of calcium spiking responses in nodulation mutants of *Medicago truncatula*. Proc Natl Acad Sci USA 97: 13407-13412

Walker SA, Viprey V, Downie AJ (2000) Dissection of nodulation signaling using pea mutants defective for calcium spiking induced by Nod factors and chitin oligomers. Proc Natl Acad Sci USA 97: 13413- 13418

Weerasinghe RR, Mck. Bird D, Allen NS (2005) Root knot nematodes and bacterial Nod factors elicit common signal transduction events in *Lotus japonicus.* PNAS 102: 3147- 3152

Weerasinghe RR, Collings BA, Johannes E, Allen NS (2003) The distributional changes and role of microtubules in Nod factor challenged in *Medicago sativa* root hairs. Planta 218: 276-287

White PJ (2000) Calcium channels in higher plants. Biochim Biophys Acta 146S: 171-189

White PJ, Broadley MR (2003) Calcium in plants. Ann Bot 92: 487-511

Williamson VM, Gleason CA (2003) Plant-nematode interactions. Curr Opin Plant Biol 6: 327-333

Zielinski RE (1998) Calmodulin and calmodulin binding proteins in plants. Annu Rev Plant Physiol Plant Mol Biol 46: 697-725